Monkeys exhibit human-like gaze biases in economic decisions

Shira M. Lupkin[1,2] & Vincent B. McGinty[1,2]

1. Center for Molecular and Behavioral Neuroscience, Rutgers University - Newark

2. Behavioral and Neural Sciences Graduate Program, Rutgers University - Newark

Correspondence: Vincent B. McGinty, vince.mcginty@rutgers.edu, 197 University Ave, Newark, NJ 07102

Acknowledgements: W.T. Newsome for funding, material support, and thoughtful discussions; A. Rangel, F. Molter, G. Rosenbaum, G. Karpov, E. Murray, D. Sharma, & A. Thomas for thoughtful discussions and comments on the manuscript; J. Brown, E. Carson, S. Fong, A. McCormick, M. Ortiz, J. Powell, J. Sanders, & D. Siegel for technical assistance. R. Kiani for creation of the ROME toolbox. F. Molter and A. Thomas for creation of the *glambox* toolbox.

Funding: S.M.L was supported by the Behavioral and Neural Sciences Graduate Program, the Rutgers University Academic Advancement Fund, and a Dean's Dissertation Fellowship. V.B.M was supported by the Howard Hughes Medical Institute (W.T. Newsome), National Institutes of Health Grant K01-DA-036659-01 (V.B.M.), the Busch Biomedical Foundation (V.B.M.), and the Whitehall Foundation (V.B.M.).

Author contributions: VBM designed the study; SML and VBM performed the research. SML and VBM analyzed the data. SML and VBM wrote the paper.

Abstract

In economic decision-making individuals choose between items based on their perceived value. For both humans and nonhuman primates, these decisions are often carried out while shifting gaze between the available options. Recent studies in humans suggest that these shifts in gaze actively influence choice, manifesting as a bias in favor of the items that are viewed first, viewed last, or viewed for the overall longest duration in a given trial. This suggests a mechanism that links gaze behavior to the neural computations underlying value-based choices. In order to identify this mechanism, it is first necessary to develop and validate a suitable animal model of this behavior. To this end, we have created a novel value-based choice task for macaque monkeys that captures the essential features of the human paradigms in which gaze biases have been observed. Using this task, we identified gaze biases in the monkeys that were both qualitatively and quantitatively similar to those in humans. In addition, the monkeys' gaze biases were well-explained using a sequential sampling model framework previously used to describe gaze biases in humans—the first time this framework has been used to assess value-based decision mechanisms in nonhuman primates. Together, these findings suggest a common mechanism that can explain gaze-related choice biases across species, and open the way for mechanistic studies to identify the neural origins of this behavior.

Introduction

Economic decisions are ubiquitous in the natural world, and in natural settings humans and other primates often evaluate the available options by moving their eyes, rapidly shifting the focus of their gaze between the options as they deliberate. Over the past decade, studies in humans have documented an association between gaze and value-based choices. In particular, when offered a choice between multiple items, people are more likely to select the first item that they view, the item they look at just prior to indicating their decision, and the item that they spend the longest time viewing over the course of their deliberation. Further, choice biases can be induced through manipulations of gaze (Gwinn et al., 2019; Liu et al., 2020, 2021; Pärnamets et al., 2015; Sui et al., 2020; Tavares et al., 2017). Together, these studies suggest that gaze plays an active role in the decision process, such that simply viewing a given option makes us more likely to choose it (see Krajbich, 2019, for a review).

However, despite increased interest in the role of gaze in decision-making, knowledge of the underlying neural mechanisms is still limited (c.f., Krajbich et al., 2021; Lim et al., 2011). One critical barrier to identifying these mechanisms is the lack of a suitable animal model of this behavior, and consequently a lack of studies addressing neural mechanisms at the cellular level. To this end, the aim of the present study was two-fold: first, to develop a novel behavioral paradigm for macaque monkeys that captures the essential features of tasks previously used in humans; and second, to determine whether monkeys exhibit gaze-based choice biases that are similar to those of humans.

While the neural mechanisms linking gaze and economic choice are not fully known, the underlying computations have been explored using sequential sampling models, a highly successful class of models used to explain simple decision behaviors (Ratcliff & McKoon,

2008). In these models, a stream of noisy evidence for each option is accumulated until one item accrues enough evidence to reach a pre-defined threshold, and a decision is rendered in favor of that item. For value-based tasks, the evidence accumulation rate can be formulated as a function of the relative value of the possible outcomes—the larger the difference in relative value, the faster that evidence accumulates for the higher-valued item. Over the last decade, the basic sequential sampling model framework has been extended to account for the influence of gaze behavior (i.e., overt attention) on the decision process. These models, collectively referred to as attentional sequential sampling models (aSSMs), assume that evidence for a given item accumulates at a faster rate while that item is being viewed, and accumulates slower when it is not being viewed (Krajbich et al., 2010; Krajbich & Rangel, 2011; Smith & Krajbich, 2018; Tavares et al., 2017; Thomas et al., 2019). Overall, these models have been successful in accounting for human gaze biases across several decision-making domains (Krajbich, 2019; Manohar & Husain, 2013; Smith & Krajbich, 2018; Thomas et al., 2019; Westbrook et al., 2020), supporting the idea that gaze modulates the decision process by biasing an evidence accumulation process.

To identify candidate neural substrates, intracranial recordings in nonhuman primates (NHPs) are an ideal approach, as they combine an animal model with human-like oculomotor behavior with the high temporal resolution necessary to accommodate the rapid pace of natural eye movements (Kravitz et al., 2013; Öngür & Price, 2000; Wise, 2008). Moreover, NHPs are commonly used as animal models in neuroeconomics. However, existing paradigms contain elements that make them unsuitable for testing the relationship between gaze and choice behavior. More specifically, many NHP studies restrict eye movements and/or use eye movements as a means of reporting choice, rather than for inspecting the choice options, (c.f.,

Cavanagh et al., 2019; Hunt et al., 2018; Rich & Wallis, 2016). These common restrictions can interfere with natural gaze patterns and therefore limit the ability to identify the relationship between gaze behavior and choice.

To address the need for an animal model of gaze biases, we have developed a novel behavioral paradigm in which monkeys are able to freely deploy their gaze to the targets on the screen and to indicate their choice by a manual response. Using this paradigm, we replicated the three core behavioral signatures of gaze-related choice biases: We found that the monkeys were more likely to choose the first item that they viewed, the last item that they viewed before deciding, and the items that received more overall gaze time. In addition, we use a computational model previously used to assess human gaze biases (Thomas et al., 2019) to determine whether similar computational mechanisms can explain choices in NHPs.

Results

Basic Psychometrics

We trained two monkeys to perform a value-based decision task in which they used eye movements to view the choice options and used a manual response lever to indicate their decision (Figure 1A). To begin a trial, the monkeys were required to fixate on the center of the task display while holding down the center of three response levers. After the required eye fixation and lever hold period was satisfied, two targets were presented on the left and right of the task display, each associated with a reward ranging from 1 to 5 drops of juice. Following the initial fixation period, gaze was unrestricted, allowing the monkeys to look at each target as many times and for as long as they liked before indicating a choice. To encourage the monkeys to look directly at the targets, and to limit their ability to perceive the targets using peripheral

vision, the targets were initially masked until the first saccade away from the central fixation point was detected (see *Methods*). To indicate their choice, the monkeys first lifted their hand off the centrally-located response lever, and then pressed the right or left lever to indicate which of the two targets they chose. The reaction time (RT) in each trial was defined as the period between the onset of the targets and the lift of the center lever. We collected data from a total of 54 sessions: 29 from Monkey C (N=15613) and 25 for Monkey K (14433).

Overall choice performance is illustrated in Figure 1D. Choices were nearly optimal for the easiest trials (value difference of +/- 3 or 4 drops of juice, > 98% of choices in favor of higher-value target) and occasionally suboptimal for more difficult trials (value difference of +/- 1 or 2 drops of juice, 86% higher-value choices for both Monkey C and Monkey K). When the targets were of equal value, the probability of the monkeys choosing the left or right target was near chance (50% left choices for Monkey C, 46% for Monkey K). This pattern of choices indicates that the monkeys were behaving according to the incentive structure of the task, with a very low rate of guesses or lapses (Fetsch, 2016). Further, choice behavior was well-described by a logistic function parameterized by the difference between the values of the left and right items (fit lines in Figure 1D are from a logit mixed effects regression: $\beta_{\text{value-difference}} = 1.37$, CI = [1.34, 1.40]; F (1,30044) = 8411.60, p < 1e-10). Additionally, we found that both the average RT and the average number of fixations per trial were modulated by choice difficulty: the monkeys responded slower and made more fixations when the two targets were near in value, compared to when the value difference between the targets was large (RT: Figure 1E, linear mixed effects regression: $\beta_{\text{difficulty}} = -0.032$, CI: [-0.039, -0.026]; F (1, 30044) = 106.09, p < 1e-10. Number of Fixations: Figure 1F, Linear mixed effects regression: $\beta_{\text{difficulty}} = -0.10$, CI = [-0.12,-0.09]; F(1, 30044) = 126.7, p < 1e-10). Together these results are consistent with behavioral patterns seen

in both humans and NHPs performing 2-alternative forced choice tasks (e.g., Gold & Shadlen, 2007; Thomas et al., 2019).

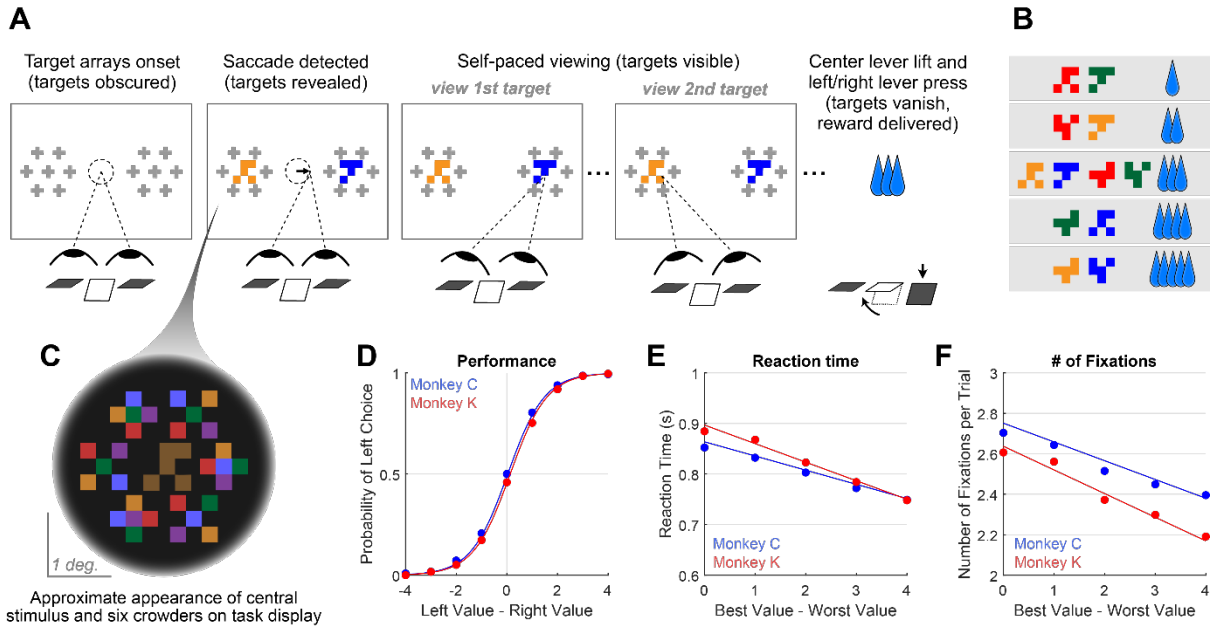

Figure 1. Decision-making task and performance in two monkeys. **A.** Abbreviated task sequence; see Figure S1 for full task sequence. The interval between target onset and center lever lift defines the decision reaction time (RT). The yellow and blue glyphs are choice targets, and the gray "+" shapes indicate the location of visual crowders designed to obscure the targets until they are viewed (fixated) directly. For clarity, in this panel crowders are shown in gray and at a reduced scale; on the actual task display, crowders were multicolored and the same size as the targets, as in panel C. **B.** An example set of 12 choice targets, organized into 5 groups corresponding to the 5 levels of juice reward. **C.** Close-up view of a single target array, consisting of a central yellow choice target surrounded by six non-task-relevant visual crowders. Two such arrays appear on the display (panel A), each located 7.5° from the display center. **D-F**. Task performance**.** **D.** Fraction of left choices as a function of the left minus right target value (in units of juice drops). **E.** Reaction Time (RT) decreases as a function of difficulty, defined as the absolute difference between target values; **F.** Number of fixations per trial decrease as a function of difficulty. Filled circles show the mean values and smooth lines show the logistic (D) or linear (E-F) regression fits derived from mixed effects models (Table 1, rows 1-3, respectively). Error bars are too small to be plotted. The data in blue are from Monkey C, and in red, from Monkey K. A subset of the data in panels D-F were reported previously in McGinty & Lupkin (2021), and the illustrations in panels A-C were adapted from McGinty & Lupkin (2021).

144 ***Effects of Difficulty and Chosen Value on Reaction Times and the Number of Fixations***

145 In the preceding section, we show both RT and the number of fixations increase as a
146 function of trial difficulty. However, in high-performing subjects trial difficulty is correlated
147 with chosen value, because the trials with large value differences (low difficulty) are also trials
148 where higher-value offers are chosen. Therefore, the RT and fixation effects originally attributed
149 to difficulty may be explained in part by chosen value. To determine the unique contributions of
150 chosen value and difficulty to RT and the total number of fixations, we used the approach of
151 Balewski and colleagues (2022). Briefly, we modeled each behavioral metric as a function of one
152 predictor, and then regressed the other predictor against the residuals of the first model. For
153 example, to measure the unique contribution of chosen value to RT, we first ran a linear mixed
154 effects model explaining RT as a function of difficulty. We then took the residuals from this
155 model, which represent the RT after accounting for difficulty, and ran a second mixed effects
156 model explaining these residuals as a function of chosen value.

157 Consistent with the findings of Balewski and colleagues, RT was modulated more by
158 chosen value than by difficulty ($\beta_{\text{chosen-value}}$ = -0.026, CI = [-0.034, -0.019]; F (1,30044) = 46.35,
159 p < 1e-10; CPD=8%; $\beta_{\text{difficulty}}$= -0.011, CI = [-0.012, -0.010]; F (1,30044) = 318.44, p < 1e-10;
160 CPD=1.4% Figure 2A/C, Table 1 rows 4-5). Interestingly, we found the opposite pattern for the
161 total number of fixations per trial: this metric was strongly modulated by difficulty ($\beta_{\text{difficulty}}$= -
162 0.065, CI = [-0.086, -0.043]; F (1,30044) = 34.46, p = 4.41e-9; CPD=1.8%; Figure 2C), and
163 showed no effect of chosen value ($\beta_{\text{chosen-value}}$ = -0.028, CI = [-0.095, 0.39]; F (1,30044) = 0.66, p
164 =0.42; CPD= 0.69%; Figure 2D, Table 1 rows 4-5). In sum RTs appear to reflect the size of the
165 upcoming reward (faster responses for higher rewards), whereas the number of fixations reflect
166 choice difficulty, with more fixations associated with more difficult trials.

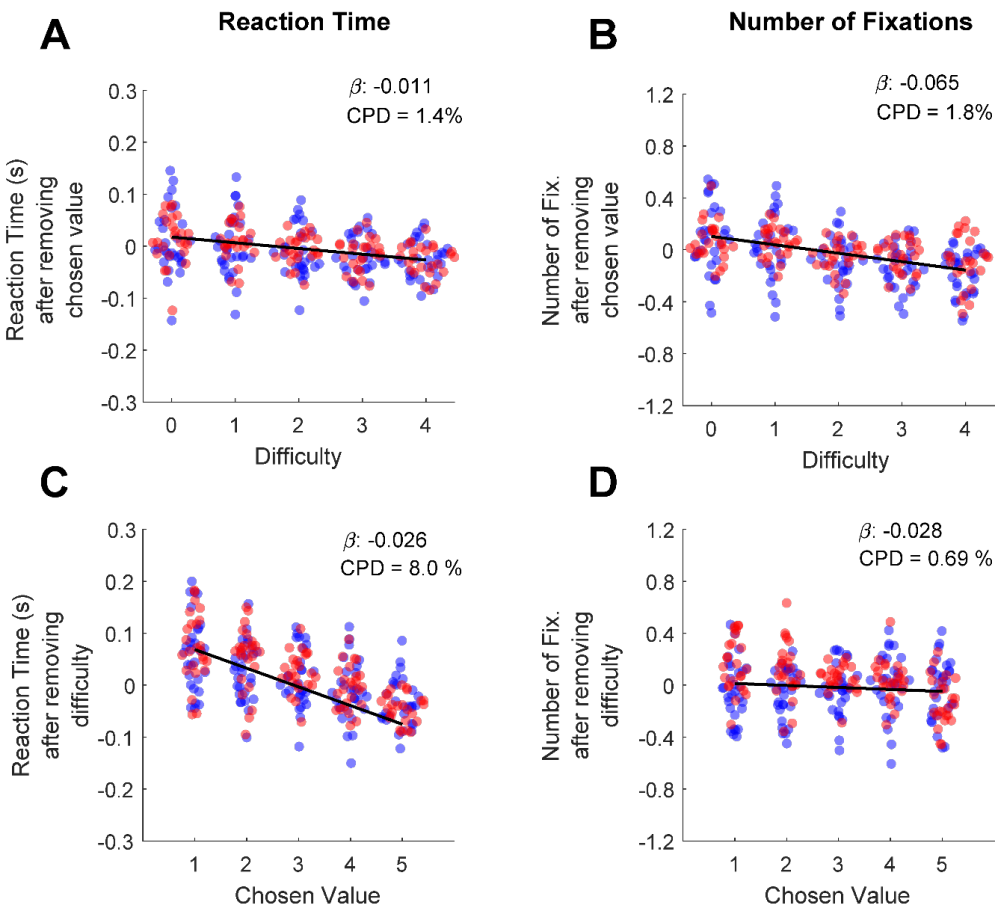

Figure 2. Differential contributions of difficulty and chosen value to decision reaction times and the number of fixations per trial. **A.** The effect of trial difficulty on reaction time after accounting for the effect of chosen value. **B.** The effect of trial difficulty on number of fixations after accounting for chosen value. **C.** The effect of chosen value on reaction time after accounting for difficulty. **D.** The effect of chosen value on number of fixations after accounting for difficulty. Y-axes give the dependent measures (RT or number of fixations) after being residualized by either difficulty or chosen value, as indicated (see Methods). Dots indicate the mean of each dependent measure for each session. Black lines show linear model fits to the plotted dots. The betas and coefficients of partial determination (CPD) of these models are in the top right corner. Blue dots are from Monkey C, red dots are from Monkey K.

Gaze Behavior and Basic Fixation Properties

The following sections characterize the number and durations of the monkeys' fixations onto the choice targets throughout each trial. A fixation was defined as a period of stable gaze upon one of the two targets. Consistent with fixation analyses in human studies, consecutive fixations upon the same target were merged into a single fixation epoch, and fixations onto non-target locations were not included in the analysis (See *Behavior Analysis* for details). Following conventions from human studies, final fixation durations are defined as the interval between fixation onset and the center lever lift; in other words, final fixation durations are delimited by the reaction time in each trial (e.g., Krajbich et al., 2010). For non-final fixations, the duration is defined in the conventional way, as the interval between fixation onset and the initiation of the next saccade.

Number of fixations per trial

In our task, information about the choice targets was obscured unless the monkey was directly fixating on them. Therefore, the optimal strategy involves a minimum of two fixations, one to each target. Consistent with this, the monkeys almost always looked at both targets on each trial (97.2% of trials for Monkey C, 91.6% for Monkey K). The fraction of trials with 1, 2, 3, or >4 total fixations before the RT for Monkey C was 2.8%, 41.2%, 49.2%, and 6.8%; and for Monkey K was 8.4%, 43.0%, 43.8%, 4.8%. Thus, in the vast majority of trials the monkeys either looked at each target exactly once (2 total fixations) or looked at one target once and the other twice (3 total fixations). The average number of fixations per trial for Monkey K was 2.45 SEM 0.02 and for Monkey C was 2.57 SEM 0.04. This average is smaller than in human binary choice tasks, in which the average number of fixations per trial is usually 3 or more. As we

discuss below, the difference between human and monkey total fixation numbers has implications for comparing fixation durations between species.

Fixation Durations Depend on Relative and Absolute Order in the Trial

Fixations can be defined by both their absolute and relative order in a trial. Absolute order refers to the serial position in the trial: first, second, third, etc. Relative order refers to when the fixation occurs with regards to the trail start or end: initial, middle, final. Note that these definitions are not independent or mutually exclusive. Instead, they depend on the total number of fixations in the trial. For example, in a trial with a total of two fixations, the second fixation is also the 'final' fixation (there are no middle fixations). However, in a trial with three total fixations, the second fixation is considered a 'middle' fixation. Because the monkeys usually make either two or three total fixations in a trial, relative and absolute order are conflated. (In contrast, humans typically make three or more fixations per trial, so that second fixations are almost always 'middle' fixations.) Consequently, it is necessary to independently analyze the effects of both absolute and relative fixation order.

To assess the effects of absolute order (first, second, third, etc.) independent of relative order (final/non-final), we first fit a linear regression explaining fixation duration as a function of relative order. We then regressed absolute order against the residuals from the first model. Consistent with human fixation patterns, we found that fixation durations decreased as a function of absolute order, after controlling for relative order ($\beta_{\text{relativeOrder}}$ = -0.049, CI= [-0.065, -0.033]; $F(1, 7762) = 36.06$, $p < 1.92e\text{-}9$; Figure 3). The decrease is especially notable at the third fixation, which in a binary task is the first 're-fixation' onto a previously sampled target, and is consistent with human fixation patterns (Manohar & Husain, 2013). Next, to assess the effects of relative order independent of absolute order, we fit a linear mixed-effects comparing fixation

218 durations across absolute positions, treating absolute position as a categorical variable. We then
219 fit a second model explaining the residuals as a function of whether or not the fixation was a
220 final fixation (i.e., relative order). After accounting for serial position, we found that non-final
221 fixations were shorter than final fixations ($\beta_{\text{relativeOrder}}$ = -0.047, CI= [-0.057,-0.037]; F(1, 7762) =
222 86.34, p < 1e-10; Figure 3). In sum, we identified two independent order-based effects on
223 duration: a decrease in duration with successive fixations in a trial, as well as a tendency to fixate
224 longer on final fixations.

225 The monkeys' prolonged final fixations seem to contradict prior human studies, which
226 typically report shorter final fixations. However, this discrepancy may be explained by the
227 relatively larger number of fixations that humans make (mean ~3.7, computed from freely
228 available data from the study described in Krajbich et al., 2010)), compared to the monkeys in
229 the present study (mean ~2.5). Consequently, humans' final fixations tend to have higher
230 absolute order and are thus nearly always re-fixations onto a target—both factors that are
231 associated with shorter fixation durations, as noted above. In contrast, the monkeys' final
232 fixations are overwhelmingly either the second or third in the trial. Thus, not only do their final
233 fixations have a lower absolute order, but they are also comprised of a larger fraction of longer
234 initial fixations onto a target (i.e., when the final fixation is the 2nd fixation).

235 ***Fixation Durations Depend on Target Value***

236 The average fixation duration was dependent on the value of the target being fixated, and
237 upon the order in the trial in which the fixation occurred. For the first fixation in each trial,
238 duration increased as a function of fixated target value (β_{fixValue} = 0.003, CI = [0.0011,0.0040];
239 F(1, 28392) = 11.37, p = 0.0007, Table 1, row 8). Intuitively, the effect size can be interpreted as
240 the influence of a one-drop change in juice volume; for example, for initial fixations the

regression estimate of 0.003 corresponds to a 3ms increase in fixation duration per drop of juice. For middle fixations, defined as any fixation that was neither first nor final, the average duration decreased as a function of the value of the fixated target ($\beta_{fixValue}$ = -0.0076, CI= [-0.0086,-0.0067]; F(1, 17580) = 231.37, p < 1e-10; Table 1, row 9). At the same time, middle fixation durations were also influenced by the value of the target not currently being viewed ($\beta_{nofixValue}$ =-0.035, CI=[-0.040, -0.030]; F(1, 17580) =197.78, p < 1e-10; Table 1, row 10; because most middle fixations were the second fixations in the trial, this means that the value of the first-viewed item "carried over" into the second fixation to influence its duration. Combining the influences of fixated and non-fixated values into a single variable, middle fixation durations increased as a function of relative value, defined here as the value of the fixated target minus the value of the non-fixated target ($\beta_{relativeFixVal}$ = 0.016, CI = [0.012, 0.021]; F(1, 17580) = 48.55, p < 1e-10; Table 1, row 11). Finally, we find that durations decreased as function of the absolute difference in target values ($\beta_{difficulty}$= -0.019, CI = [-0.025,-0.0154; F(1, 17580) = 47.17, p < 1e-10; Table 1, row 12). Together, these results support the notion that fixation behavior and valuation are not independent processes, and that the effects of value on viewing durations must be accounted for when computing and interpreting gaze biases (see *Cumulative Gaze-Time Bias*, below).

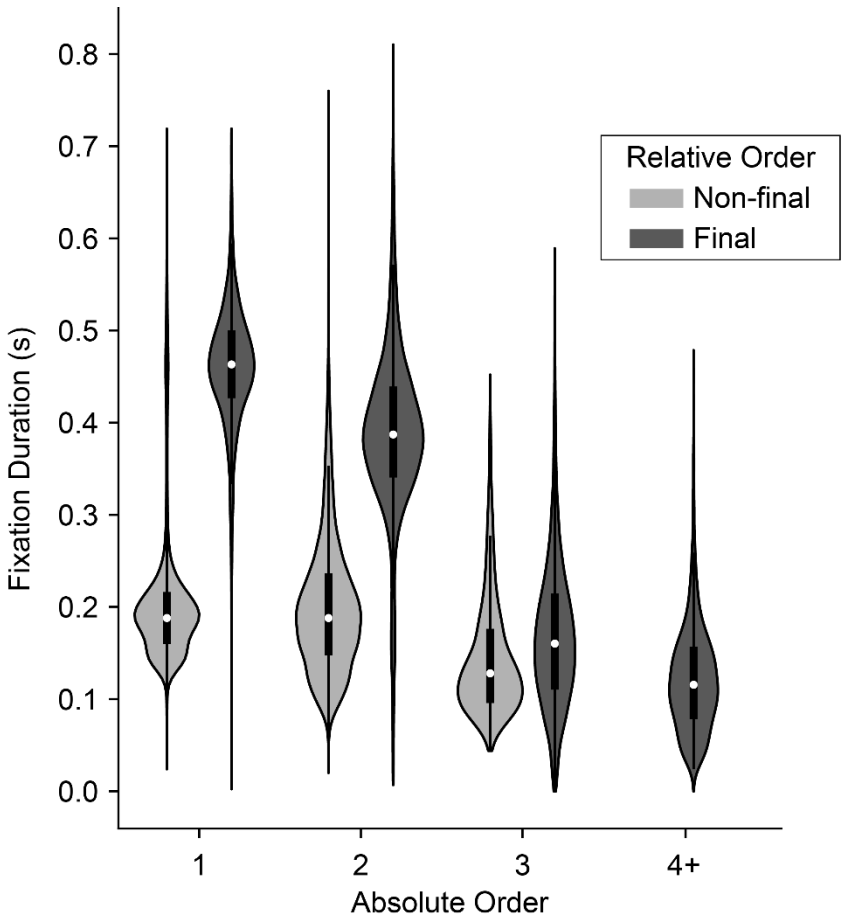

Figure 3. Distribution of fixation durations across absolute and relative position in the trial. Violins show distribution of fixation durations across absolute position in the trial (x-axis) and split according to whether they were final (dark gray) or non-final (light gray) fixations in the trial. 1st fixations: N = 30,046 non-final and 1652 final; 2nd fixations: N = 15,753 non-final and 12,641 final; 3rd fixations: N = 1,749 non-final and 14,004 final; 4th fixations or greater: N = 80 non-final (not shown) and 1,749 final.

Gaze-Related Choice Biases

Humans show three core choice biases related to gaze behavior. First, they tend to choose the item that they viewed first (initial fixation bias). Second, they tend to choose the item they spend more time looking at over the course of the trial (cumulative gaze-time bias). Third, they tend to choose in favor of the target they are viewing at the moment they indicate their choice. All three of these biases are evident in our monkey subjects, as detailed below. However, before

266 these biases can be quantified, we must first address the question of whether monkeys show
267 evidence for a two-stage form of gaze bias recently identified in human behavior.

268 ***Evidence for a Two-Stage Model of Gaze Biases***

269 To explain how these gaze biases come about, prior human studies have used modified
270 sequential sampling models (aSSMs) by providing an increase in evidence accumulation for a
271 given item while it is being viewed (see Krajbich, 2019, for review). This bias generally takes
272 one of two forms: Some studies suggest that the gaze amplifies the value of attended targets so
273 that the increase in evidence accumulation is proportional to the attended value (i.e., is
274 multiplicative). Others suggest that gaze acts by providing a fixed increase in evidence
275 accumulation to attended targets, independent of target values (i.e., is additive). Studies directly
276 comparing these two mechanisms are not fully conclusive (Smith & Krajbich, 2019; Thomas et
277 al., 2019), perpetuating debates as to which is "correct". A third, hybrid modeling framework
278 offers a compromise (Manohar & Husain, 2013; Westbrook et al., 2020). Under this framework,
279 a trial can be divided into two stages. The first stage is the decision stage, where evidence
280 accrues for the decision offers, and gaze increases evidence accumulation for attended items in
281 multiplicative fashion. The second stage begins once an internal decision boundary is reached (a
282 choice is made) and continues until the choice is physically reported. During this interval the
283 gaze becomes drawn to the to-be-chosen item, which is captured with an additive gaze bias. In
284 other words, in the first stage, gaze influences choice, whereas in the second stage, the latent
285 choice influences gaze.

286 Two patterns in the monkeys' fixation data are consistent with this two-stage model.
287 First, as shown in Figure 3, final fixation durations are longer than non-final fixations even after
288 accounting for absolute order in the trial, suggesting some process that occurs at the end of each

trial thus prolonging fixation durations. Second, the monkeys' final fixations were on the to-be-chosen target on nearly every trial (~97% of trials), consistent with gaze being drawn to the to-be-chosen items.

To more directly test the hybrid, two-stage, model in our data, we reasoned that the relative fit of a model with an additive gaze bias compared to one with a multiplicative gaze bias would indicate whether choice reflects one mechanism alone, or a mixture of both. Using the Gaze-Weighted Linear Accumulator Model (GLAM, Thomas et al. 2019), we found that while the multiplicative model provided a slightly better fit than the additive model, the difference was not significant (Figure 4, 0 on the x-axis, Table S2). This suggests that our data likely reflect a mixture of additive and multiplicative gaze biases, consistent with the hybrid model.

Next, we tested the assumption that the influence of gaze switches between the two biasing mechanisms near the end of the trial, at the moment a decision threshold is met. We reasoned that if this were the case, that relative fit of one model over the other would increase if we removed increasing amounts of data from the end of the trial. Alternatively, if the multiplicative and additive influences were mixed throughout the trial, this truncation would have little effect on the relative fit of the two model variants. We found that the difference in fit between the two models became significant for truncation values of 100ms and higher, with the multiplicative model providing the better fit (Table S2). Further, at 100ms the probability that data were generated by a multiplicative, and not an additive, model reaches 100% (Figure 4). Together, this supports the two-stage model put forth by Westbrook, where the gaze acts multiplicatively during the first stage before transitioning to additive approximately 100ms before the RT.

312 ***Estimating and Truncating the Terminal Non-decision Time***

313 Under the two-stage framework, the transition point between the multiplicative and
314 additive stages of the decision process occurs when accumulated evidence reaches the decision
315 boundary. In other words, the additive stage occurs *after* a decision has been made but before the
316 RT is detected. In standard sequential sampling models, this type of post-decision/pre-report
317 interval is referred to as terminal non-decision time (NDT; Ratcliff & McKoon, 2008; Resulaj et
318 al., 2009). As noted above, we estimated that in our data, this transition occurs approximately
319 100ms prior to the RT. Because the focus of this study was to characterize the influence of gaze
320 on the decision process itself (i.e., the putative first stage), the remaining analyses were
321 conducted using data that were truncated by 100ms, in order to minimize the influence of post-
322 decision gaze effects. However, as this is merely an estimate of the NDT interval, we repeated
323 each analysis using data truncated over a range of NDT values from 0-400ms. The results,
324 presented in supplemental Figures S2, and S3, indicate that the gaze biases described in the
325 following sections are robust to NDT truncation values of up to 200ms.
326

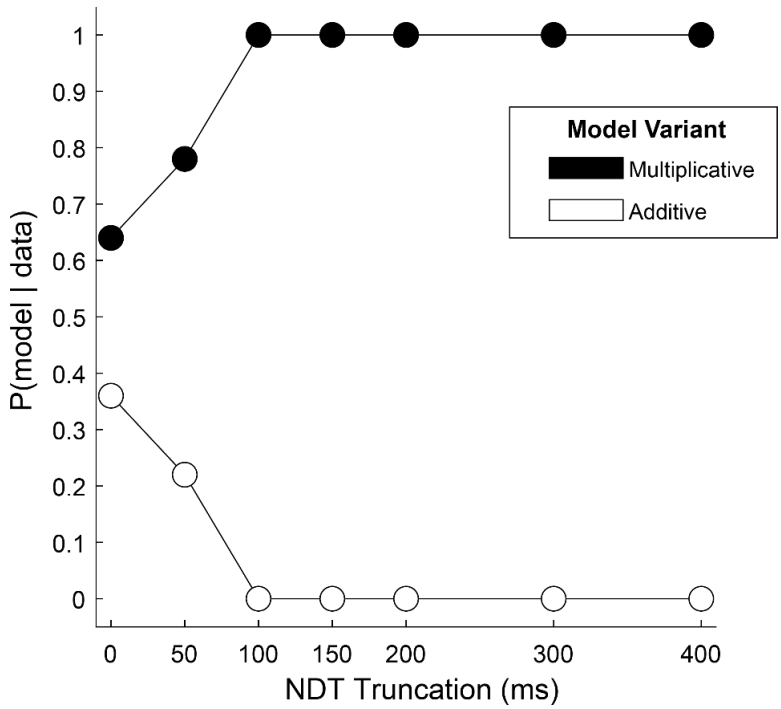

Figure 4. Relative fit of multiplicative and additive models across NDT truncation values. Using an aSSM modeling framework, we computed the posterior probability (y-axis) of a model with either a multiplicative gaze bias parameter (black circles) or an additive parameter (white circles) being more likely to have generated the data. Probabilities were computed using data in which the final portion of the trial was truncated by 0, 50ms, 100ms, etc. (x-axis) See *Estimating and truncating the terminal non-decision time* for details.

Initial Fixation Bias

As is the case in humans, the monkeys were more likely to choose the target that they looked at first in a given trial. To quantify this bias, we used a logit mixed effects regression, which gives an estimate of the effect of an initial leftward fixation on the log odds of a leftward choice: $\beta_{\text{first-is-left}} = 0.66$, CI = [0.32; 1.00]; F(1,30043) = 14.36, p = 0.00015, see Table 1, 13). The fact that $\beta_{\text{first-is-left}}$ is significantly greater than zero indicates that an initial leftward fixation is associated with a greater likelihood of a leftward choice. The effect of target value differences computed in this same model was $\beta_{\text{value-difference}} = 1.40$ (CI = [1.32, 1.43]; F (1,30043) = 5349.40, p < 1e-10). The ratio between these two regression estimates ($\beta_{\text{first-is-left}}$ / $\beta_{\text{value-difference}}$), gives the relative influence the initial fixation on choice as compared to the value differences of the

targets: 0.66/1.40 = 0.47. In other words, the monkeys chose as if the first-fixated item was, on average, worth 0.47 drops of juice more than its nominal value. Critically, because the targets were obscured until the monkeys initiated their first saccade (see *Methods*), their initial fixations were unbiased with regard to target value. Thus, the choice bias in favor of the initially fixated item cannot be attributed to a tendency for the monkeys to look at higher value targets first.

This suggests that the initial fixation direction, whether exogenously or endogenously driven, may have a causal influence in choice. To test this causal role, we conducted additional experimental sessions in which we manipulated initial fixation by staggering the onset of the two targets (Monkey C: 16 sessions, n = 6931 trials; Monkey K: 8 sessions, n = 5433 trials). Staggered target onsets – either left first or right first – occurred randomly in 30% of the trials in these sessions (Figure 3A), with concurrent onsets in the other 70% of trials (Figure 3B). In the staggered-onset trials, the monkeys almost always directed their initial fixations to the target that appeared first (100% of staggered trials for Monkey C, 94.1% for Monkey K). Trials in which the Monkey K did not fixate on the first target (n = 99) were removed from analysis. As in the sessions without gaze manipulation described above, we found a main effect of initial fixation on choice (logit mixed effects regression: $\beta_{\text{first-is-left}}$ = 0.70, CI = [0.41; 1.00]; F(1,12359) = 21.83, p = 3.02e-06; $\beta_{\text{first-is-left}}$ / $\beta_{\text{value-difference}}$ = 0.57 drops of juice; see Figure 5 and Table 1, row 14). Importantly, we found no main effect of trial-type (staggered vs. standard; $\beta_{\text{trial-type}}$ = -0.07, CI = [-0.33; 0.18]; F(1,12359) = 0.32, p = 0.57) nor was there a difference in the magnitude of the initial fixation effect across the two trial-types $\beta_{\text{first-is-left:trial-type}}$ = 1.48e-3, CI = [-0.23; 0.24]; F(1,12359) = 1.52e-4, p = 0.57). Thus, not only could we induce an initial fixation bias by manipulating where the monkey looked first, but the magnitude of this bias is comparable to the bias observed without a manipulation.

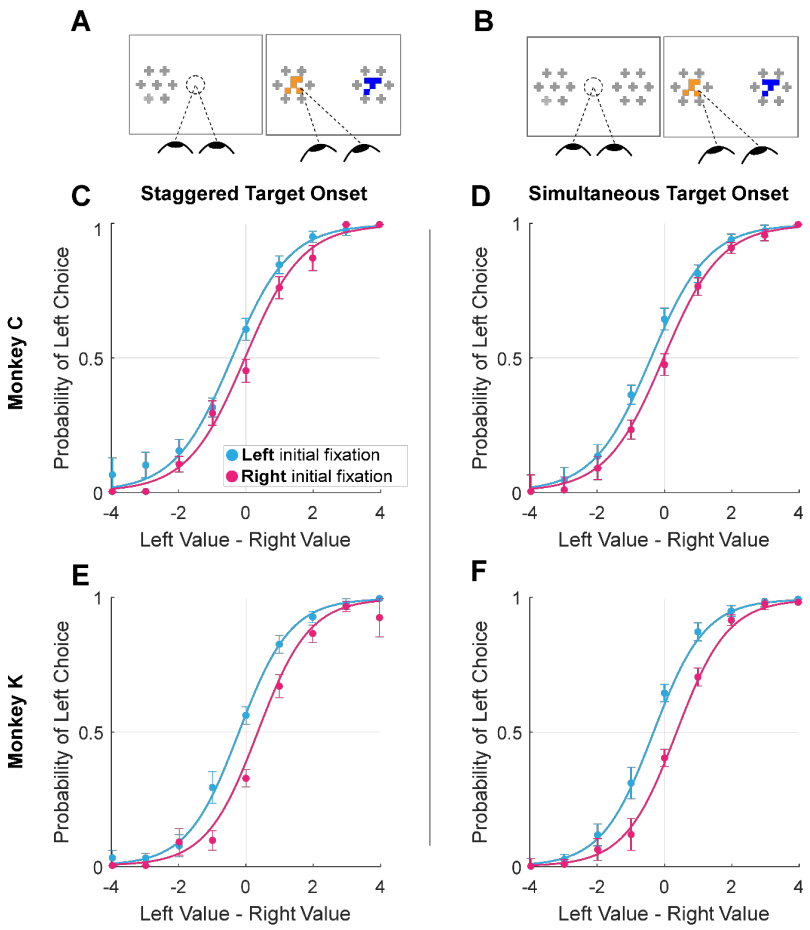

Figure 5. Initial gaze bias for gaze-manipulation sessions. A. Depiction of gaze manipulation procedure. In 30% of trials, only a single target was initially presented, randomly assigned to the left or right of the display (left panel). Once a saccade was detected (or 250ms elapsed, whichever happened first), the second target appeared (right panel). **B.** Depiction of standard trials with masked targets appearing simultaneously on both the left *and* right of the display (left panel). Masks disappeared when the initial saccade was detected (right panel). **C-F.** Probability of choosing left as a function of the difference between the value of the item on the left and the value of the item on the right. Data were split according to the direction of the initial fixation (cyan and magenta) Circles show the mean probabilities of left choice, error bars show the standard error of the mean over 16 sessions for Monkey C and 8 sessions for Monkey K. Lines show logistic fits from the mixed effects model (Table 1, row 13). **C & E**. show data from trials where the onset of the first target was staggered. **D & F.** show trials where the targets appeared simultaneously. **C-D.** shows data from Monkey C; **E-F.** shows data from Monkey K.

363 ***Cumulative Gaze-Time Bias***

364 Here, we asked whether monkeys were more likely to choose items that were fixated
365 longer in a trial. We first quantified the time spent looking at the two choice targets in every trial.
366 Then, using a logit mixed effects regression, we asked whether choice outcomes were dependent
367 on the relative time spent looking at the left item as compared to the right item ("Time
368 Advantage Left"). Consistent with human choice patterns, monkeys were more likely to choose
369 the left item as the relative time advantage for the left item increased (Figure 6B,C; $\beta_{\text{time-advantage}}$
370 =18.71, CI = [15.07; 22.34]; F(1,28393) = 101.76, p < 1 e- 10, Table 1, row 15). Because
371 fixation durations are themselves dependent upon the target values (see *Fixation Durations*
372 *Depend on Target Value*, above), we repeated this analysis using choice probabilities that were
373 corrected to account for the target values (see *Methods*). Using these corrected choice
374 probabilities, the positive relationship between relative viewing times and choice was
375 maintained. (Figure 6D,C; linear mixed effects regression: $\beta_{\text{time-advantage}}$ = 1.07, CI = [0.92;
376 0.1.21]; F(1, 28393) = 208.90, p < 1 e- 10, Table 1, row 16). Intuitively, this effect size would
377 predict a change in choice probability of ~5% given a change in relative viewing time advantage
378 from -0.1s to 0.1s. Thus, the monkeys were more likely to choose items that were fixated longer,
379 independent of the values of the targets in each trial. The corrected cumulative gaze time bias
380 effects were significantly above zero for data truncated up to 200ms (Fig. S2).

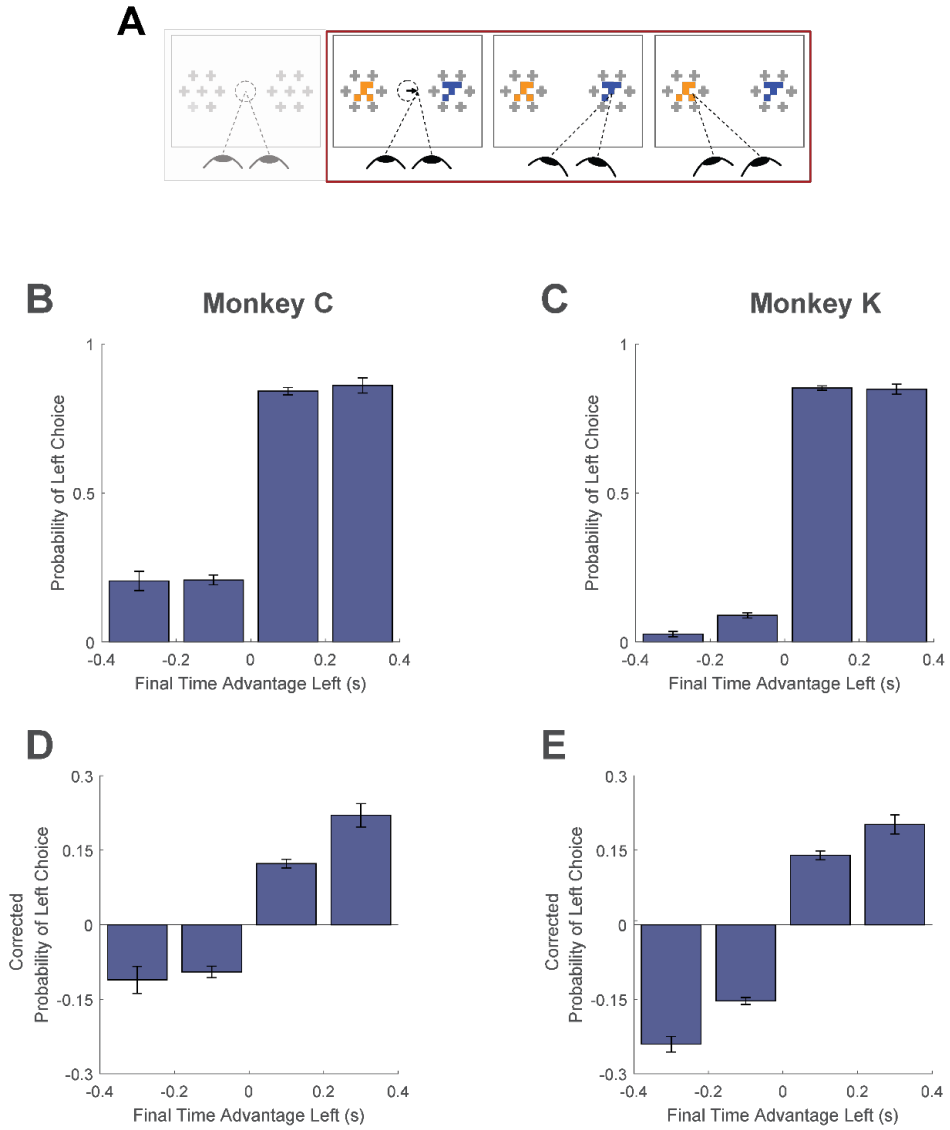

Figure 6. Cumulative gaze-time bias. A. Task schematic. The portion of the trial used to show the cumulative gaze-time bias is highlighted in red. **B-C.** Probability of choosing left as a function of the binned final gaze-bias advantage for the left item. **D-E.** The same as B-C**,** but using choice probabilities corrected to account for the target values in each trial (see *Methods*). For visualization, these graphs exclude those trials with a final time advantage greater than +/- 3 standard deviations from the mean (< 1% of trials for each monkey). The trials were not excluded from the logit mixed effects regression reported in the text. In B-E, the bin boundaries were 0, ±0.2, and ±∞. Error bars indicate SEM across sessions.

384 ***Final Fixation Bias***

385 A prediction of earlier aSSM models is that the item being fixated at the end of the trial
386 should be chosen more often than the non-fixated item, due to the net increase in evidence
387 accumulation for fixated items, and consequently the greater likelihood that evidence for a
388 fixated item reaches a bound at any given moment. (Krajbich et al., 2010; Krajbich & Rangel,
389 2011; Tavares et al., 2017). In contrast, the two-stage model described by Westbrook and
390 colleagues (2020), suggests that the final fixation reflects, rather than influences, the result of the
391 accumulation process. Therefore, we assessed the final fixation bias in our data in a manner
392 similar to prior studies but with one important difference: as detailed above, the fixation data in
393 each trial were truncated by 100ms to minimize the influence of late-stage gaze effects. In the
394 truncated data, the location of the final fixation in each trial is defined as the target being viewed
395 by the monkey at the *virtual* end of the trial, which in an aSSM framework can be interpreted as
396 an estimate of when the decision boundary was reached (e.g., Resulaj et al., 2009).

397 Using the truncated data, we found that the monkeys were more likely to choose the
398 target being viewed at the virtual trial end, consistent with the final fixation bias effects observed
399 in humans (Figure 7, logit mixed effects regression: $\beta_{\text{last-is-left}} = 3.35$, CI = [2.34; 4.37];
400 $F(1,28392) = 42.00$, $p < 1e\text{-}10$, Table 1, row 17). Note that this effect is present even after
401 removing up to 200ms from the end of the trial (approximately 25% of the full trial duration,
402 Figure S3). This means that final fixation biases can be explained at least in part by an effect of
403 gaze on evidence accumulation – as suggested by prior studies (Krajbich et al., 2010)– when
404 assuming a terminal NDT epoch of up to 200ms.

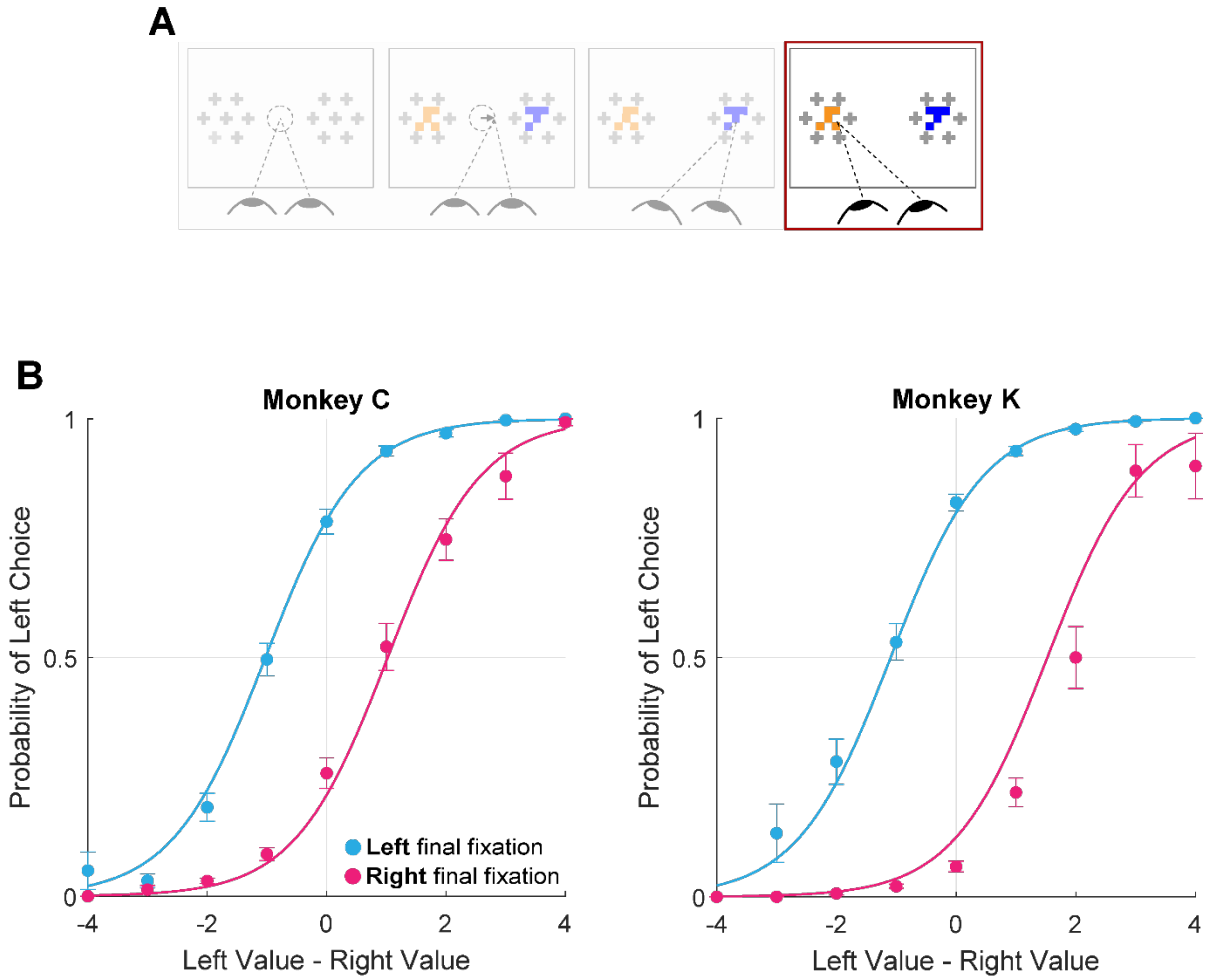

Figure 7. Final Fixation Bias. A. Task schematic highlighting the portion of the trial used to show the final fixation bias (red box). **B-C.** Probability of choosing left as a function of the difference in item values, split according to the location of gaze (left or right) at the end of the trial. Circles show mean probabilities of left choice, error bars show the standard error of the mean over 25 sessions for Monkey C and 29 sessions for Monkey K. Lines show logistic fits from the mixed effects model (Table 1, row 17). Panel B shows data from Monkey C; panel C shows data from Monkey K.

405

Gaze-Weighted Linear Accumulator Model (GLAM)

The analyses above show broad consistency between NHP and human data with respect to the association between gaze and choice behavior. The question remains, however, as to whether these patterns emerge from a similar mechanism to those observed in humans. To this end, we asked whether an aSSM framework could explain the gaze and choice patterns we observed in NHPs. We chose the Gaze-weighted Linear Accumulator Model (GLAM; Molter et al., 2019), which was previously used to explain gaze-related choice biases in humans across multiple independent decision studies (Thomas et al., 2019). Using this model, we asked three questions with regards to our NHP data: First, does a model with a gaze bias mechanism fit our data better than a similar model without a gaze bias? Second, how do gaze biases estimated in our monkey subjects compare to prior human work? Third, can the model accurately predict the critical features of choice behavior, such as accuracy, RT, and the influence of gaze on choice? To answer the first question, we fit two variants of the GLAM to each monkeys' data. These variants differed only in their treatment of the gaze bias parameter, γ (see Equation 1 for model specification and parameter definitions). Note that since the model was fit using the NDT-truncated data, we exclusively utilized the multiplicative version of the model (See Figure 4 and associated text). In the first GLAM variant, the gaze bias parameter γ was left as a free parameter, allowing gaze to modify the rate of evidence accumulation for fixated items. The second model fixed γ at 1, assuming *a priori* that gaze has no effect on the decision process. The maximum a posteriori (MAP) and 95% highest posterior density intervals (HPD) for the parameters estimated in both model variants are given in Table S1. The relative fit of the two variants was assessed using the difference in WAIC score (dWAIC, Vehtari et al., 2017), defined by subtracting the WAIC value for the model with γ fixed at 1 from the WAIC for the model

where γ was a free parameter. The dWAIC for Monkey C was -3357.9, and for Monkey K was -8159.7, indicating that the model that allowed for the presence of gaze biases is the better fit of the two model variants. Further, this difference was significant as indicated by nonoverlapping WAIC values ± their standard error (Table S1). In the gaze-bias model, γ values were as follows: Monkey C: MAP=0.079, HPD= [0.045, 0.12]; Monkey K: MAP = -0.056, HPD = [-0.087, -0.018].

Since the GLAM had previously been used to explore gaze biases in four human decision-making datasets (Folke et al., 2016; Krajbich et al., 2010; Krajbich & Rangel, 2011; Tavares et al., 2017), we were able to directly compare the extent of the gaze bias by comparing the γ parameters for humans vs. our monkey subjects. Treating each session as an independent sample, we found that the distribution of γ in each of our monkey subjects fully overlapped with the γ distributions from human studies (Figure 8).

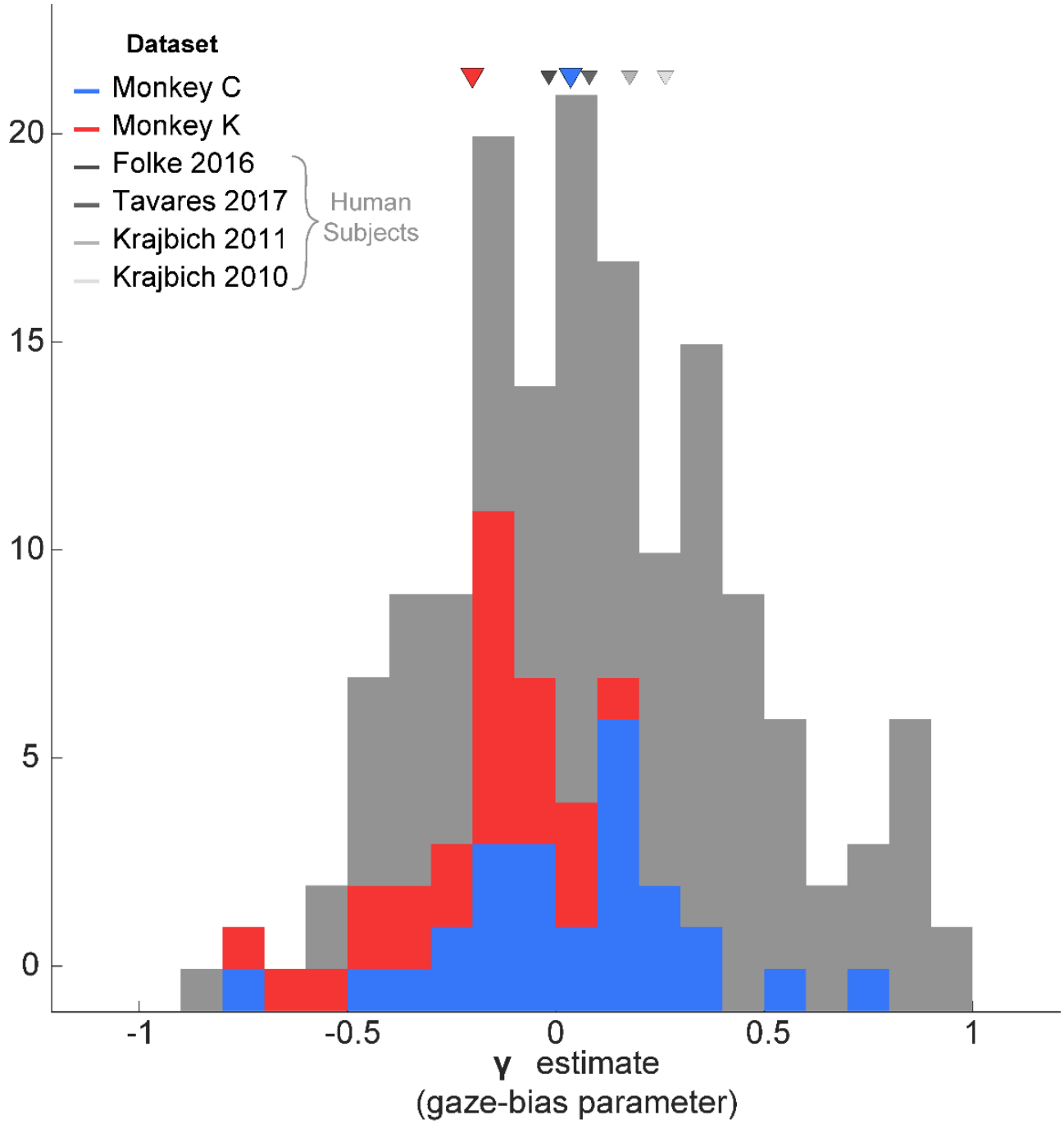

Figure 8. Distribution of gaze bias parameter (γ) across species. X-axis shows the range of possible values of the gaze bias parameter, γ. The gray distribution combines the γ values estimated for each subject in the four human datasets previously fit using the GLAM (Thomas et al., 2019). The means for each dataset are given as triangles above the distributions. The blue and red distributions show the session-wise distribution of γ parameters for Monkeys C, and K, respectively. Triangles in the corresponding colors show the means of the monkeys' distributions. Total number of subjects for each dataset are as follows: Folke, 2016: 24 subjects; Tavares, 2017: 25 ; Krajbich, 2011: 30; Krajbich, 2010: 39. Total number of sessions for the monkeys were 29 and 25 for Monkeys C and K, respectively.

Finally, we assessed the model's predictive accuracy by performing out-of-sample simulations to predict core features of the behavioral data. To do this, the data were first split into even- and odd-numbered trials. Next, the models were estimated using only the even-numbered trials. Finally, these estimates were used to simulate each of the held-out trials 10 times, resulting in a set of simulated choice and reaction time measures that could be compared to the empirically observed behavior in the held out trials. As illustrated in Figure 9, the model predictions closely match the monkeys' actual performance (see also Table 1, rows 18-20 and Table S3). Note that repeating this procedure with γ fixed at 1 (no gaze bias) produces accurate predictions of choices and reaction times but fails to capture the effect of cumulative gaze-bias on choice (not illustrated, see Thomas et al., 2019).

In summary, an aSSM model that includes gaze bias provides a better fit than a model without a gaze bias, and that the magnitude of this bias is comparable to that estimated in human data using the same modeling framework. Finally, the model is able to make accurate out-of-sample predictions of choice and gaze behavior.

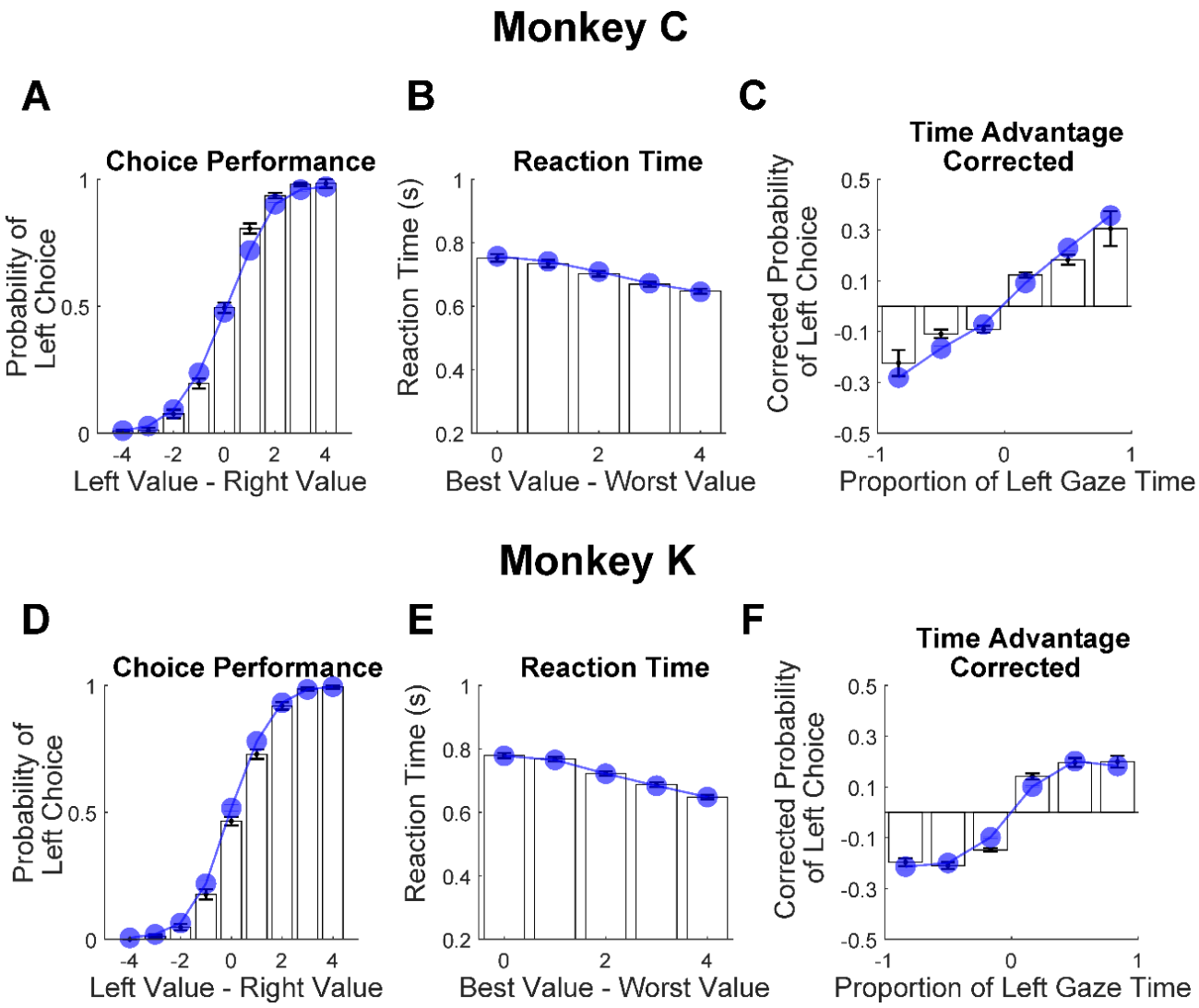

Figure 9. Out-of-sample predictions of the GLAM model for choice and gaze behavior. White bars show the empirically observed behavioral data from monkeys in odd-numbered trials. Blue dots and lines show GLAM model predictions for odd-numbered trials. Error bars show the standard error of the mean across sessions (SEM). **A,D.** Fraction of left choices as a function of the left minus right target value (in units of juice drops). **B,E.** Reaction time decreases as a function of difficulty; note that reaction times are shorter here than in Figure 1E, due to the use of NDT-truncated data. **C,F.** Corrected probability of choosing the left target as a function of the fraction of time spent looking at the left target minus fraction of time spent looking at the right target. The bin boundaries are 0, ±0.33, ±0.67, and ±1. Panels A-C correspond Monkey C; panels D-F correspond to Monkey K.

Discussion

Over the last decade, there has been a growing appreciation for the active role that attention plays in a broad array of decision-making domains. However, the neural substrates of this relationship remain largely unknown due to the lack of a suitable animal model. The aim of the present study was to develop such a model using a novel value-based decision-making task for NHPs. We validated our animal model on two measures: behavioral control and the presence of human-comparable gaze biases. First, the monkeys' performance indicated good behavioral control: both choices and RTs were a graded function of task difficulty (defined by the difference in target values), with fast and nearly optimal choices in the easiest trials, and slower and more variable choices in harder trials. Such signatures of behavioral control are crucial to the development of any animal model of complex cognitive processes, as they allow the confident attribution of an animal's behavior to the construct of interest, and not to attentional lapses or guesses (Fetsch, 2016; Krakauer et al., 2017). For the present study, this suggests that the monkeys' behavior is ascribable to a decision process driven primarily by the values of the targets in each trial. As to the second criterion, our results show that the monkeys exhibit similar gaze biases to those observed humans, both in terms of the core behavioral measures and also in their ability to be mechanistically described using an aSSM. Taken together, this novel task is well suited for use in neural mechanistic studies, such as concurrent electrophysiological recordings or stimulation.

Comparison to Prior Human Studies

While our findings are broadly consistent with those from humans, there are two notable differences between the monkeys' gaze behavior in the present study, and that of humans reported in prior studies. First, monkeys made fewer fixations per trial than humans on average

(~2.5 vs. 3.7); second, the monkeys' final fixations in each trial tended to be prolonged compared to non-final fixations—the opposite of what has been reported in many human studies. Critically, these two differences may be related. For both humans and monkeys, fixations made early in the trial are longer than those made later; thus, because the monkeys' final fixations occur early in the trial (e.g. either 2nd or 3rd), they will be longer on average than final fixations in humans, which tend to occur later in the trial (e.g. 4th, 5th, etc.).

One significant similarity between the current study and prior studies in humans was the positive association between gaze and choices, which was well-explained using an aSSM. As noted in the results, our data are most consistent with a two-stage aSSM in which gaze initially biases the choice process, and then (after a decision boundary is reached) transitions to a mode in which gaze becomes drawn to the intended choice target (Manohar & Husain, 2013; Westbrook et al., 2020). The behavioral feature of this second stage is consistent with a motor-preparatory phenomenon known as a gaze-anchoring, in which gaze becomes 'locked' onto the reach target in order to increase the speed and efficiency of the response (Battaglia-Mayer et al., 2001; Dean et al., 2011; Neggers & Bekkering, 2000).

In prior studies of gaze-anchoring in humans and NHPs, the latency between the eyes locking onto target of an upcoming response and the beginning of detected movement ranges between 64-100ms (Battaglia-Mayer et al., 2001; Neggers & Bekkering, 2001, 2000; Reyes-Puerta et al., 2010; Stuphorn et al., 2000). The terminal NDT estimate that we derived from the model comparison is consistent with these latencies, and with NDT estimates obtained from standard sequential sampling models (e.g., Resulaj et al., 2009). Ultimately, the true duration of the post-decision epoch is difficult to estimate from behavioral data alone. Additional work will

be necessary to either measure or infer the plausible range of post-decision/pre-report intervals in our task, in order to confirm the robustness of the gaze bias effects measured here.

Comparison to Prior NHP Studies

Beyond similarities to prior human studies, our results are also consistent with the handful of NHP studies in which some degree of free eye movement was permitted. Among these, both Hunt et al., 2018 and Rich & Wallis, 2016 imposed some restrictions on eye movements, making it difficult to assess the relationship between fully natural gaze patterns and choices. Cavanagh and colleagues (2019) used a fully free-viewing design, and also observed a bias in favor of initially fixated items.

Our study confirms this result, and provides additional insights, due to novel elements of the study design. First, by manipulating initial fixation direction, we show that initial fixation has a causal effect on the decision process. Second, the results of the aSSM model-fitting provide a mechanistic explanation for our results and permits a direct comparison to model fitting results in human studies.

Finally, unlike many prior studies, the decision task requires the monkeys to sample the targets by fixating them directly, due to the use of a gaze contingent mask that completely obscures the stimuli at the beginning of the trial, and the use of visual crowders that closely surround each target. This subtle design element is crucial, because it permits accurate measurement of the time spent attending to each target, and of the relationship between relative viewing time and choice. In a forthcoming study using this same task, we show that OFC neurons do not begin to reflect the value of the second-fixated stimulus until well after it has been viewed by the monkey, indicating that value information is only available to the monkey once a target is fixated (McGinty & Lupkin, 2021). In contrast, in tasks where value-associated

529 targets are easily perceived in peripheral vision, even targets that are not fixated influence
530 prefrontal value signals and decision behavior (e.g., Cavanagh et al., 2019; Xie et al., n.d.).
531 High-value peripheral targets are also implicated in value-based attentional capture, in which
532 overt or covert attention becomes drawn to objects that are reliably associated with reward
533 (Anderson et al., 2011; Kim et al., 2015). Thus, the task used in the present study minimizes
534 value-based capture effects.

535 **Hypothesized Neural Substrates**

536 The impetus for developing this animal model is to explore the neural underpinnings of
537 the relationship between gaze and value-based choice. Given the fact that a sequential sampling
538 model provides objectively good fits to the observed behavior, one potential approach for
539 understanding neural mechanisms is to identify brain regions that correspond to different
540 functions in a sequential sampling framework. Such an approach has been used in perceptual dot
541 motion discrimination, where extrastriate cortical area MT is thought to provide the "input"
542 signal (encoding of visual motion) and neurons in parietal area LIP are thought to represent the
543 accumulated evidence over time (see Gold & Shadlen, 2007, for review). One note of caution,
544 however, is that brain activity that outwardly appears to implement accumulator-like functions
545 may not be causally involved in the choice (e.g. Katz et al., 2016). Nonetheless, it is still useful
546 to consider the neural origins of two core computations suggested by sequential sampling
547 models: the representation of the target values (corresponding to the input signals), and neural
548 signals that predict of the actions performed to obtain the reward (reflecting the decision output).

549 For the encoding of accumulated evidence, findings from NHP neurophysiology point to
550 regions involved in the preparation of movement. In motion discrimination tasks that use eye
551 movements to report decisions, accumulated evidence signals can be observed in oculomotor

control regions such as area LIP, frontal eye fields, and the superior colliculus. Because the decision in our task is reported with a reach movement, potential sites for accumulator-like activity include motor cortical areas such as the arm representations within dorsal pre-motor cortex (Chandrasekaran et al., 2017). In addition, human imaging studies have identified several other candidate regions with accumulator-like activity, including in the intraparietal sulcus, insula, caudate, and lateral prefrontal cortex (Gluth et al., 2012; Hare et al., 2011; Pisauro et al., 2017; Rodriguez et al., 2015). Interestingly, several studies find accumulator-like signals in cortical areas in the dorsal and medial frontal cortex, but these are not consistently localized. For example, whereas Pisauro et al. (2017) find accumulator-like activity in the supplementary motor area, Rodriguez et al. (2015) identify a more anterior region in the medial frontal cortex. Additional studies in both humans and NHPs will be necessary to understand the specializations of these regions with respect to encoding decision evidence.

Because decision behavior in this study was value-dependent, regions encoding economic value are strong candidates for signals that provide input to an accumulator. Value-related signals have been observed in numerous cortical and subcortical regions, including the amygdala (e.g., Paton et al., 2006), the ventral striatum (Kable & Glimcher, 2009; Lim et al., 2011), and the ventromedial frontal lobe (VMF), including both the orbitofrontal and ventromedial prefrontal cortices (Padoa-Schioppa & Assad, 2006; Rich & Wallis, 2016; Vaidya & Fellows, 2015). Of these regions, the VMF has received the most scrutiny with regards to gaze-biases. In humans, there is evidence of BOLD activity in this region related to attention-guided decision-making (Gluth et al., 2012; Hare et al., 2011; Leong et al., 2017; Lim et al., 2011; Pisauro et al., 2017; Rodriguez et al., 2015), and patients with lesions to this area show impairments in such tasks (Vaidya & Fellows, 2015).

575 In NHPs, the orbitofrontal portion of the VMF (the OFC) has been demonstrated to
576 contain value-signals that are dependent on whether gaze is directed towards a reward-associated
577 visual target (Hunt et al., 2018; McGinty et al., 2016; McGinty & Lupkin, 2021) a mechanism
578 fully consistent with the effects of gaze posited by aSSM frameworks. However, the precise
579 neural mechanisms explaining how gaze biases choice outcomes are still unknown. One
580 hypothesis is that the value-coding regions inherit gaze-modulated information from visual
581 cortical regions sensitive to shifts in visual attention. For instance, neurons in the anterior
582 inferotemporal cortex, which projects directly to the OFC (Carmichael & Price, 1995; Kravitz et
583 al., 2013), selectively encode features of attended objects to the exclusion of others in the same
584 receptive field (DiCarlo and Maunsell, 2000; Moore et al., 2003; Moran and Desimone, 1985;
585 Richmond et al., 1983; Sheinberg and Logothetis, 2001). Therefore, the similar fixation-driven
586 effects on OFC value-coding shown by McGinty and colleagues (McGinty et al., 2016; McGinty
587 & Lupkin, 2021) may be inherited from this structure. Another candidate region for the top-down
588 influences on gaze-dependent value-coding, is the frontal eye fields (FEF). In a recent study from
589 Krajbich et al. (2021), focal disruption of FEF leads to a reduction in the magnitude of gaze-
590 biases. Prior work in both humans and NHPs has shown that the FEF can influence perceptual
591 sensitivity through the top-down modulation of early visual areas (Moore & Armstrong, 2003;
592 Moore & Fallah, 2004; Ruff et al., 2006; Silvanto et al., 2006; Taylor et al., 2007), suggesting
593 that it may exert similar influence on value-encoding regions.

594 **Conclusions**

595 In real-world decision scenarios, both humans and NHPs depend heavily on active visual
596 exploration to sample information in the environment and make optimal decisions. In this way,
597 even simple decisions require dynamic sensory-motor coordination. The importance of these

gaze dynamics is underscored by the growing number of human studies showing that gaze systematically biases the decision process. We have developed a novel value-based decision-making task for macaque monkeys and found that monkeys spontaneously exhibit gaze biases that are quantitatively similar to humans', while also showing the high level of behavioral control necessary for neurophysiological study. This novel paradigm will therefore make it possible to identify the cell- and circuit-level mechanisms of these biases.

621 **Methods**

622 **Subjects**

623 The subjects were two adult male rhesus monkeys (*Macaca Mulatta*), referred to as
624 Monkey C and Monkey K. Both subjects weighed between 13.5 and 15kg during data
625 acquisition, and both were 11 years old at the start of the experiment. They were implanted with
626 an orthopedic head restraint device under full surgical anesthesia using aseptic techniques and
627 instruments, with analgesics and antibiotics given pre-, intra-, and post-operatively as
628 appropriate. Data from Monkey K were collected at Stanford University (25 sessions, 14433
629 trials); data from Monkey C were collected at Rutgers University—Newark (29 sessions, 15613
630 trials). All procedures were in accordance with the Guide for the Care and Use of Laboratory
631 Animals (2011) and were approved by the Institutional Animal Care and Use Committees of
632 both Stanford University and Rutgers University—Newark.

633 **Study Design and Apparatus**

634 The subjects performed the task while head-restrained and seated in front of a fronto-
635 parallel CRT monitor (120Hz refresh rate, 1024x768 resolution), placed approximately 57cm
636 from the subjects' eyes. Eye position was monitored at 250 Hz using a non-invasive infrared eye-
637 tracker (Eyelink CL, SR Research, Mississauga, Canada). Three response levers (ENV- 612M,
638 Med Associates, Inc., St. Albans, VT) were placed in front of the subjects, within their reach.
639 The "center" lever was located approximately 17cm below and 35cm in front of the display
640 center, and the center points of the two other levers were approximately 9cm to the left and right
641 of the center lever. The behavioral paradigm was run in Matlab (Mathworks, Inc., Natick, MA)
642 using the ROME toolbox (R. Kiani, 2012). Juice rewards were delivered through a sipper tube
643 placed near the subjects' mouths.

Behavioral Task

Task Structure

Figure 1A shows an abbreviated task sequence; Figure S1A shows the full sequence as described here: Each trial began with a fixation point in the center of the screen. Upon appearance of the fixation point, the subjects were required to both depress the center lever and to maintain fixation within a radius of 3.5 degrees of visual angle from the center of the fixation point. The monkeys were required to use only one hand to perform the task (Monkey K used his right hand; Monkey C used his left). After the initial fixation and center lever press were both held for an interval between 1-1.5 seconds, the fixation point disappeared, and two target arrays were presented 7.5 degrees to the left and right of the fixation point. Each target array consisted of a choice target, an initial mask, and six non-relevant "visual crowders". The net effect of the mask and crowders was to obscure the target until the monkey looked directly at the target with a saccadic eye movement. See *Gaze Contingent Mask and Visual Crowders,* below, for details. The two targets shown in each trial were selected randomly without replacement from a set of 12 (see Figures 1B & S1C) and placed randomly on the left or right side of the display, giving 132 unique trial conditions.

Once the target arrays appeared, the monkeys were free to move their gaze as they desired and were free to initiate a choice at any time. To initiate a choice, the monkeys lifted their hand off the center lever, at which point the target arrays were extinguished. After releasing the center lever, the monkeys had 500 or 400ms (for Monkey C and K, respectively) to choose their desired target by pressing the left or right lever. After a delay (1s for Monkey K; 1 or 1.5s for Monkey C), the subjects received the volume of juice reward associated with the chosen target (range 1-5 drops). If neither the left nor right lever was pressed within 400 or 500ms of

667 the center lever lift, the trial ended in an error. Each trial was followed by an inter-trial interval
668 randomly drawn from a uniform distribution between 2 and 4 seconds. Eye movements
669 following the initial fixation were monitored but not enforced, and had no programmatic
670 influence on the outcome of the trial. Reaction time (RT) was calculated as the time between
671 target arrays onset and the release of the center lever.

672 ***Choice Targets***

673 Choice targets were constructed as composites of two features, color and shape, and the
674 reward value of a given target (range 1-5 drops) was determined by the sum of the reward values
675 associated with its two features. (Figure S1C). Notably, this scheme allows for multiple visually
676 distinct targets to share the same value. An example target set is shown in Figure 1B and Figure
677 S1C. For a given set, the colors were selected by randomly sampling four equally-spaced hues
678 from a standardized color wheel based on the CIELUV color space, and shapes were quasi-
679 randomly selected from a library of 28 equal-area shapes.

680 New stimulus sets were generated frequently to avoid over-training on a given stimulus
681 set. For every new set, 1-2 training sessions (not used for analysis) were performed so that the
682 monkeys could become familiar with the stimuli, followed by 1-3 sessions of data collection.

683 ***Gaze-Contingent Initial Mask and Visual Crowders***

684 A key design goal of this task was to encourage the monkeys to fixate onto the choice
685 targets directly using saccadic eye movements. To encourage this behavior, we used two
686 methods to obscure the choice targets until they were fixated directly.

687 The first method was a gaze-contingent initial mask: when the target arrays first appeared
688 in each trial (i.e. the first frame), the choice targets were not shown; rather, in their place were
689 two non-relevant, non-informative masking stimuli-drawn from a pool of visual crowder stimuli

690 (described below). The masking stimuli remained until the monkeys' moved their eyes out of the
691 initial fixation window by initiating a saccade, usually ~150ms after the onset of the arrays. Once
692 the eyes left the initial window, the masking stimuli were replaced with the actual choice targets
693 in the next display frame. Because the display frame rate (one frame every 8.25ms) was shorter
694 than the typical time taken to complete a saccade (~30-40ms), the switch from the masks to the
695 actual stimuli occurred while the monkeys' eyes were moving, so that the choice targets
696 appeared on the display before the end of the saccade (See Figure S1A for a step-by-step
697 illustration). Therefore, information about target values was only available after the monkeys
698 initiated a saccade towards one of the two target arrays.

699 The second method was the use of 6 visual crowders placed in close proximity in a
700 hexagonal arrangement around each target (Figure 1C). These crowders minimized the monkeys'
701 ability to use peripheral vision to identify the choice targets (Crowder & Olson, 2015; Whitney
702 & Levi, 2011), further encouraging them to make fixations directly onto the targets.

703 The initial mask stimuli and the visual crowders were constructed using plus (+) or cross
704 (x) shapes, colored using five hues randomly sampled from equally spaced points on a
705 standardized color wheel. These stimuli convey no value information because the plus and cross
706 shapes were never used to construct target stimulus sets, and because the use of multiple, random
707 hues within each of the stimuli does not signify any one color that could indicate value.

708 The crowders and initial target masking were highly effective at encouraging the
709 monkeys to fixate both targets before initiating a choice: both targets were viewed in 97.2% of
710 trials for Monkey C and 92.6% of trials for Monkey K. These methods also ensured that the first
711 fixation following target onset was unbiased with respect to the target values: in trials where one
712 target had a larger value than the other, the monkeys directed their first saccade towards the

713 higher value target 49.9% of the time, which was not significantly different from chance
714 (t (25559) = -0.45, p = 0.65).

715 **Gaze Manipulation**

716 To test the causal nature of the relationship between initial fixation and choice, we
717 conducted additional sessions in which we temporally staggered the onset of the two targets.
718 (Monkey C: 16 sessions, n = 6931 trials; Monkey K: 8 sessions, n = 5433 trials). During these
719 sessions, in 30% of the trials the first target array would appear randomly on either the left or
720 right of the screen. The second target array appeared 250ms after the onset of the first, or when
721 the monkeys began their initial saccade away from the central fixation point, whichever came
722 first. The location of the first target array was randomized across trials. This manipulation was
723 intended to encourage the monkeys to direct their attention towards the target that appeared first,
724 as shown in prior human studies (Tavares et al., 2017). As expected, the monkeys directed their
725 initial fixation to the cued target on 96% of the staggered-onset trials.

726 **Behavioral Analysis**

727 With the exception of the computational modeling, analyses were performed in Matlab v.
728 R2022a (Mathworks, Inc., Natick, MA). All graphs, except Figure 3, were generated within the
729 Matlab environment. For Figure 3, the violin plots were generated using the Seaborn v. 0.12.2
730 library for Python (Waskom, 2021). Unless otherwise noted, analyses were conducted using
731 generalized mixed-effects regressions with random effects for monkey-specific slopes and
732 intercepts. To fit these models, data were collapsed across sessions, unless otherwise noted. Full
733 specifications for all models are given in Table 1. Regression estimates (β's) and 95 %
734 confidence intervals (CI) are reported for each effect. Significance for each effect was

determined using a post-hoc ANOVA in which the regression estimates were compared to 0 (*F*- and *p*- values, reported in the text).

The onset and duration of fixations, defined as periods of stable gaze upon one of the two targets, were recorded by the Eyelink CL software. For analysis purposes, a fixation was considered to be on a given target if it was located within 3-5 degrees of the target center. Two consecutive fixations made onto the same target were merged into one continuous fixation. Fixations that were not onto either target were discarded; however, these were extremely rare: in the vast majority of trials, the monkeys fixated exclusively upon the targets.

For analysis purposes, fixations were designated as “first”, “final” or “middle”. First fixations were defined as the first target that was fixated after the onset of the target arrays; final fixations were defined as the target being fixated at the moment the monkey initiates a choice by lifting the center lever; and middle fixations were defined as all on-target fixations that were neither first nor final. Fixation durations were measured in the conventional manner, except for final fixations, which were considered to be terminated at the time of choice in each trial, consistent with previous human studies (Krajbich et al., 2010; Krajbich & Rangel, 2011; Tavares et al., 2017; Westbrook et al., 2020). When using truncated data (see *Estimation and Truncation of Terminal Non-Decision Time (NDT), below)* final fixations were terminated at the virtual trial end point.

For analyses of the final fixation bias and the cumulative gaze-time bias, trials containing only a single fixation were excluded (Monkey C: N = 447 trials (2.8% of total), Monkey K: N = 1217 trials (8.4% of total)), as they could artificially inflate either or both of these biases. For the latter analysis, we computed in every trial the time advantage for the left item by subtracting the total duration of fixations onto the right target from the total duration of fixations onto the left

target (Krajbich et al., 2010). Thus, for trials where the monkey allocated more gaze time to the left target, the time advantage takes a positive value, whereas it takes a negative value for trials where the monkey allocated more gaze time to the right.

Finally, for the cumulative gaze bias analyses shown in Figure 6D and 6E, choice proportions were corrected using the same procedure set forth in Krajbich et al., 2010. For each trial, we coded the choice outcome as 0 for a right choice and 1 for a left choice. Then from each trial's choice outcome we subtracted the average probability of choosing left for all trials in that same condition, where the condition was defined as the left minus right target values. This correction removes from the choice data any variance attributable to the differences in the target values; as a result, Figure 4C and 4E reflect the effect of cumulative gaze after accounting for the influence of the target values on gaze durations.

	Behavioral Effect	Regressors	Equation(s)	Figure(s)
	Basic Psychometrics			
	Basic Psychometrics			
1	Choice (Left = 1, Right = 0) x Value Difference	Value Difference	Choice ~ logit(value-difference)	1D
2	Reaction Time (RT) x Difficulty	Difficulty	RT ~difficulty	1E
3	Number of Fixations (Num. Fix.) x Difficulty	Difficulty	Num. Fix. ~difficulty	1F
	Contributions of Difficulty and Chosen Value on RT and Fixations			
4	Independent Contribution of Chosen Value (DV = RT or Num. Fix)	Chosen Value (chosen-value) Difficulty	Model 1: DV ~difficulty Model 2: ResidModel1 ~ chosen-value	2A/B
5	Independent Contribution of Difficulty (DV = RT or Num. Fix)	Chosen Value (chosen-value) Difficulty (difficulty)	Model 1: DV ~ chosen-value Model 2: ResidModel1 ~ difficulty	2C/D
	Gaze Behavior and Basic Fixation Properties			
	Fixation Durations Depend on Relative and Absolute Order in the Trial			
6	Independent Effect of Absolute Order	Relative Order (Final = 1, Non-Final = 0; relativeOrder) Absolute Order (1st, 2nd, etc.; absoluteOrder)	Model 1: Fixation Duration ~ relativeOrder Model 2: ResidModel1 ~ absoluteOrder	3
7	Independent Effect of Relative Order	Absolute Order (1st, 2nd, etc.; absoluteOrder) Relative Order (Final = 1, Non-Final = 0; relativeOrder)	Model 1: Fixation Duration ~ categorical(absoluteOrder) Model 2: ResidModel1 ~ relativeOrder	3
	Fixation Durations Depend on Target Value			
8	Initial Fixation Duration x Fixated Target Value	Value of Fixated Target (ValueFixated)	Initial Fixation Duration ~ fixValue	-
9	Middle Fixation Duration x Fixated Target Value	Value of Fixated Target (ValueFixated)	Middle Fixation Duration ~ fixValue	-
10	Middle Fixation Duration x Not-Fixated Target Value	Value of Non-Fixated Target (nofixValue)	Middle Fixation Duration ~ nofixValue	-
11	Middle Fixation Duration x Relative Target Value	Relative Target Value (relativeFixVal)	Middle Fixation Duration ~ relativeFixVal	-
12	Middle Fixation Duration x Difficulty	Difficulty	Middle Fixation Duration ~ difficulty	-
	Gaze-Related Choice Biases			
	Initial Fixation Bias			
13	Standard Sessions	Value Difference Initial Fixation Location (1 =Left, 0 = Right; first-is-left)	Choice ~ logit(value-difference + first-is-left)	-
14	Gaze Manipulation Sessions	Value Difference Initial Fixation Location Trial-Type (1 = staggered, 0 = simultaneous; trial-type)	Choice ~ logit(value-difference + first-is-left + trial-type + first-is-left:trial-type	5
	Cumulative Gaze-Time Bias			
15	Standard Choice	Left Time Advantage (time-advantage)	Choice ~ logit(time-advantage)	6B/C
16	Value-Corrected Choice	Left Time Advantage	Value-Corrected Choice ~ time-advantage	6D/E
	Final Fixation Bias			
17	Final Fixation Bias	Value Difference Final Fixation Location (1 =Left, 0 = Right; last-is-left)	Choice ~ logit(value-difference + last-is-left)	7
	Gaze-Weighted Linear Accumulator Model			
	Out-of-Sample Goodness-of-Fit			
18	Choice	isSimulated (simulated trial = 1, observed trial = 0)	Choice ~ logit(isSimulated)	9A/D
19	RT	isSimulated (simulated trial = 1, observed trial = 0)	RT ~ isSimulated	9B/E
20	Value-Corrected Choice	isSimulated (simulated trial = 1, observed trial = 0)	Value-Corrected Choice ~ isSimiluated	9C/F

Table 1. Mixed effects model specifications. *All models included a monkey-specific slope and intercept for each effect. In line 14, the asaterisk indicathe addition of a term for each variable, as well as the interaction between them.*

Computational Model

To gain insight into potential mechanisms underlying choice and gaze behavior in this task, we employed the Gaze Weighted Linear Accumulator Model (GLAM, Thomas et al., 2019). The GLAM modeling was conducted in Python version 3.7 using the *glambox* toolbox (see *Code Availability* for details). The GLAM is an aSSM characterized by a series of parallel accumulators racing to a single bound. These accumulators are co-dependent, such that their combined probability of reaching the bound is equal to 1. For two choice options, this formulation is mathematically equivalent to a single accumulator drifting between two bounds (Thomas et al., 2019, Krajbich et al., 2011). The effect of gaze on choice behaviors is implemented as follows: The GLAM posits that over the course of a trial the absolute evidence signal for each item, i, can have two states: a biased state during periods when an item is viewed, and an unbiased state when it is not. The average absolute evidence for each item, A_i, is a linear combination of these two states throughout the trial. As noted in the results, there are two methods through which gaze could be biasing choice behavior: a multiplicative manner in which gaze amplifies the value of the attended target, and an additive manner in which gaze adds a fixed increase in evidence accumulation to the attended target, independent of its value.

Assuming a multiplicative bias, A_i is defined according to Equation 1a.

$$A_i = g_i r_i + (1 - g_i)\,\gamma r_i \quad \text{(Eqn. 1a)}$$

Here, r_i is the veridical value of target i (number of drops of juice), g_i is the fraction of gaze time that the monkey devoted to that target during a given trial, and γ is the crucial gaze bias parameter, which determines the extent to which the non-fixated item is discounted. This

792 parameter has an upper bound of 1, which corresponds to no gaze bias. A value of γ less than 1
793 indicates biased accumulation in favor of the fixated item.

794 Under an additive gaze-biasing mechanism, A_i is defined according to equation 1b.

795 $$A_i = r_i + \gamma g_i \quad \text{(Eqn. 1b)}$$

796 As in the multiplicative model, r_i is the veridical value of target i (number of drops of juice), g_i is
797 the fraction of gaze time that the monkey devoted to that target during a given trial, and γ is the
798 gaze bias parameter. However, in the additive model variant, a γ value of 0 corresponds to no
799 gaze bias, and a nonzero γ value indicates biased accumulation in favor of the fixated item.

800 The gaze-adjusted absolute evidence signals for each item are then used as inputs to an
801 evidence accumulation process, as follows: First, each absolute value signal (A_i) is converted to
802 a relative evidence signal, R_i, through a logistic transform (see Molter et al., 2019; Thomas et al.,
803 2019 for details and rationale). Then, evidence for each item (E_i) at time t is accumulated
804 according to Equation 2, where ν and σ indicate the speed of accumulation and the standard
805 deviation of the noise, respectively, and R_i is the relative evidence signal. N indicates a univariate
806 normal distribution. A choice is made when the evidence for one of the items reaches the
807 threshold.

808 $$E_i(t) = E_i(t-1) + vR_i + N(0, \sigma^2);\ E_i(0) = 0 \quad \text{(Eqn. 2)}$$

809 We fit several different variants of the GLAM model to each monkey's data. To evaluate
810 a hybrid two-stage modeling framework, we compared the relative fit of multiplicative and
811 additive models to the data (Figure 4). Given the overall better fit obtained from the
812 multiplicative models, these were used for the remainder of the analyses. To evaluate the
813 necessity of the gaze bias parameter γ for explaining behavior, we used two variants of the
814 multiplicative model, one in which the gaze bias parameter was left as a free parameter, and

another that assumed no gaze bias by setting $\gamma = 1$ (results in reported in Table S1). Model fits were compared using the Widely Applicable Information Criterion (WAIC, Vehtari et al., 2017) which accounts for the differences in the complexity of the two model variants. Specifically, we used both the signed difference of WAIC values and the WAIC weights for each model, which can be interpreted as the probability that each model is true, given the data (Vehtari et al., 2017).

In addition, we assessed the model's predictive accuracy by estimating the parameters for the free- γ model variant using only even numbered trials, and then using these parameter estimates to simulate the results of each of the held-out odd-numbered trials 10 times. We quantified the goodness-of-fit of the simulations by comparing three outcome metrics: choice, RT, and corrected probability of a leftward choice as a function of the cumulative gaze time advantage for the left item (as in Fig. 4D, E). Note that since value is removed from the corrected cumulative gaze effect metric (see above), the only input to the model that could modulate it was the relative amount of gaze time devoted to each target. Thus, we can use this metric to assess the model's ability to emulate the net effect of gaze alone on choice. For each metric we computed a mixed effects regression (logistic for choice, linear for RT and the corrected cumulative gaze effect), in which a vector including both the empirically observed data and the simulations was explained as a function of a binary variable indicating whether a data point came from the empirically observed data, or from the model simulations (i.e., *Metric ~ 1 + isSimulated*). If the fixed effect of this variable was not significantly different from 0, then the simulated data did not deviate from the empirically observed data. The mean deviations for each metric are given by the beta-weights and are reported in Table S3 along with the confidence intervals. As with the other regression models used in this paper, "Monkey" was included as a random effect.

All GLAM parameter estimation procedures were identical to those set forth in Thomas et al., 2019, with one exception: Thomas and colleagues assumed a fixed rate of random choice of 5%. This was changed to 1% to reflect the extremely low lapse rate for the easiest trials shown by both monkeys. The lapse rate for each monkey was estimated by finding the percentage of trials in which the monkey chose a 1-drop target when a 5-drop target (the highest possible value) was also available (mean lapse rate: Monkey C = 0.64%, Monkey K = 0.33%).

Estimation and Truncation of Terminal Non-Decision Time (NDT)

In sequential sampling models, the interval between when a decision is reached and when it is detectable to the experimenter is referred to as non-decision time (NDT). To account for and minimize the influence of gaze behavior in this interval, we truncated the gaze data using an estimate of this post-decision epoch. To obtain this estimate, we leveraged the key assumption of the two-stage aSSM, namely that gaze acts in a multiplicative manner prior to a boundary crossing (i.e., reaching a latent decision) and then additively between the boundary crossing and when the decision is reported (i.e., the RT, Manohar & Husain, 2013; Westbrook et al., 2020) Therefore, by removing gaze data from the end of the trial, the probability of the data being better explained by an additive model (and not a multiplicative model) should decrease as more data are removed. We collapsed data across the two monkeys and fit both an additive and a multiplicative variant of the GLAM for data truncated at 0ms, 50ms, 100ms, 150ms, 200ms, 300ms, and 400ms. We then compared the posterior probabilities of the model being correct given the data and the alternative model using the *compare* function from PyMC. We also compared the WAIC for the two variants, for each level of truncation (Figure S2 & S3, Table S3). The relative probability of the additive model generating the data decreases sharply between 0ms and 100ms of truncation, after which it reaches zero.

Accordingly, we selected 100ms as our NDT estimate, and for the data shown in the main figures removed gaze data between center lever lift and 100ms before the lever lift in every trial. In other words, in every trial the gaze data were treated as if the trial had actually ended 100ms before the center lever lift; all calculations related to the gaze sequence and timing were calculated with respect to this virtual trial stopping point. For trials where the virtual stopping point occurred during an earlier fixation, we reassigned the final fixation location according to the location of the eyes at the virtual stopping point. In this way, the effects of late-trial gaze effects during the NDT were minimized. The truncated data were used to compute the gaze biases, except the initial fixation bias, and were also used as input to the computational model. Importantly, the main analyses were repeated using truncation values ranging from 0-400ms, with results shown in Figures S2 & S3.

Sample Size Determination

Because the behavioral task was novel, and because there were no published data from free-viewing NHP decision tasks at the time the study began, there were no effect size estimates available to facilitate a power analysis. We therefore began by collecting a pilot sample, and assessing the initial gaze bias and cumulative gaze bias effects as reported in humans by Krajbich et al. (2010). To minimize confirmatory bias stemming from exploratory analyses, these initial analyses procedures were identical to those in Krajbich et al. The first pilot sample, in Monkey K, consisted of 13 sessions (approximately 8000 trials). Using planned analyses from Krajbich et al., we identified statistically significant initial fixation and corrected cumulative gaze biases. Based upon this initial sample, we then targeted a per-monkey sample size of approximately 10-15 sessions or 7,000-15,000 trials for detecting behavioral effects of interest in subsequent experiments.

We then collected additional sessions from Monkey K for the purposes of electrophysiological recordings. These were combined with previous behavior-only sessions to create the Monkey K data used in this study (total = 25 sessions). From the second monkey we first collected 13 behavior-only sessions, and then additional 16 sessions for the purpose of electrophysiological recordings, resulting in the 29 sessions for Monkey C reported here. We defined outlier sessions as those in which the fraction of suboptimal decisions exceeded ~1% for the easiest choices (+/- 3 or 4 on the X-axis in Figure 1D), indicating that the monkeys had not yet sufficiently learned the target values; these sessions were excluded from analysis. No exclusions were made on the basis of gaze data, or upon gaze-related outcome measures.

Code Accessibility

The data and code in this folder are available at https://osf.io/hkgmn/. The *glambox* toolbox that was used for the computational modeling can be accessed at https://github.com/glamlab/glambox. The associated documentation can be accessed at https://glambox.readthedocs.io/en/latest/.

References

Anderson, B. A., Laurent, P. A., & Yantis, S. (2011). Value-driven attentional capture. *Proceedings of the National Academy of Sciences*, *108*(25), 10367–10371. https://doi.org/10.1073/pnas.1104047108

Balewski, Z. Z., Knudsen, E. B., & Wallis, J. D. (2022). Fast and slow contributions to decision-making in corticostriatal circuits. *Neuron*. https://doi.org/10.1016/j.neuron.2022.04.005

Battaglia-Mayer, A., Ferraina, S., Genovesio, A., Marconi, B., Squatrito, S., Molinari, M., Lacquaniti, F., & Caminiti, R. (2001). Eye–Hand Coordination during Reaching. II. An Analysis of the Relationships between Visuomanual Signals in Parietal Cortex and Parieto-frontal Association Projections. *Cerebral Cortex*, *11*(6), 528–544. https://doi.org/10.1093/cercor/11.6.528

Carmichael, S. T., & Price, J. L. (1995). Sensory and premotor connections of the orbital and medial prefrontal cortex of macaque monkeys. *Journal of Comparative Neurology*, *363*(4), 642–664.

Cavanagh, S. E., Malalasekera, W. M. N., Miranda, B., Hunt, L. T., & Kennerley, S. W. (2019). Visual fixation patterns during economic choice reflect covert valuation processes that emerge with learning. *Proceedings of the National Academy of Sciences*, *116*(45), 22795–22801. https://doi.org/10.1073/pnas.1906662116

Crowder, E. A., & Olson, C. R. (2015). Macaque monkeys experience visual crowding. *Journal of Vision*, *15*(5), 14–14. https://doi.org/10.1167/15.5.14

Dean, H. L., Martí, D., Tsui, E., Rinzel, J., & Pesaran, B. (2011). Reaction Time Correlations during Eye–Hand Coordination: Behavior and Modeling. *Journal of Neuroscience*, *31*(7), 2399–2412. https://doi.org/10.1523/JNEUROSCI.4591-10.2011

Fetsch, C. R. (2016). The importance of task design and behavioral control for understanding the neural basis of cognitive functions. *Current Opinion in Neurobiology*, *37*, 16–22. https://doi.org/10.1016/j.conb.2015.12.002

Folke, T., Jacobsen, C., Fleming, S. M., & De Martino, B. (2016). Explicit representation of confidence informs future value-based decisions. *Nature Human Behaviour*, *1*(1), Article 1. https://doi.org/10.1038/s41562-016-0002

Gluth, S., Rieskamp, J., & Büchel, C. (2012). Deciding When to Decide: Time-Variant Sequential Sampling Models Explain the Emergence of Value-Based Decisions in the Human Brain. *Journal of Neuroscience*, *32*(31), 10686–10698. https://doi.org/10.1523/JNEUROSCI.0727-12.2012

Gold, J. I., & Shadlen, M. N. (2007). The Neural Basis of Decision Making. *Annual Review of Neuroscience*, *30*(1), 535–574. https://doi.org/10.1146/annurev.neuro.29.051605.113038

Gwinn, R., Leber, A. B., & Krajbich, I. (2019). The spillover effects of attentional learning on value-based choice. *Cognition*, *182*, 294–306. https://doi.org/10.1016/j.cognition.2018.10.012

Hare, T. A., Schultz, W., Camerer, C. F., O'Doherty, J. P., & Rangel, A. (2011). Transformation of stimulus value signals into motor commands during simple choice. *Proceedings of the National Academy of Sciences*, *108*(44), 18120–18125. https://doi.org/10.1073/pnas.1109322108

Hunt, L. T., Malalasekera, W. M. N., de Berker, A. O., Miranda, B., Farmer, S. F., Behrens, T. E. J., & Kennerley, S. W. (2018). Triple dissociation of attention and decision computations across prefrontal cortex. *Nature Neuroscience*, *21*(10), 1471–1481. https://doi.org/10.1038/s41593-018-0239-5

Kable, J. W., & Glimcher, P. W. (2009). The Neurobiology of Decision: Consensus and Controversy. *Neuron*, *63*(6), 733–745. https://doi.org/10.1016/j.neuron.2009.09.003

Katz, L. N., Yates, J. L., Pillow, J. W., & Huk, A. C. (2016). Dissociated functional significance of decision-related activity in the primate dorsal stream. *Nature*, *535*(7611), Article 7611. https://doi.org/10.1038/nature18617

Kim, H. F., Ghazizadeh, A., & Hikosaka, O. (2015). Dopamine Neurons Encoding Long-Term Memory of Object Value for Habitual Behavior. *Cell*, *163*(5), 1165–1175. https://doi.org/10.1016/j.cell.2015.10.063

Krajbich, I. (2019). Accounting for attention in sequential sampling models of decision making. *Current Opinion in Psychology*, *29*, 6–11. https://doi.org/10.1016/j.copsyc.2018.10.008

Krajbich, I., Armel, C., & Rangel, A. (2010). Visual fixations and the computation and comparison of value in simple choice. *Nature Neuroscience*, *13*(10), 1292–1298. https://doi.org/10.1038/nn.2635

Krajbich, I., Mitsumasu, A., Polania, R., Ruff, C. C., & Fehr, E. (2021). A causal role for the right frontal eye fields in value comparison. *ELife*, *10*, e67477. https://doi.org/10.7554/eLife.67477

Krajbich, I., & Rangel, A. (2011). Multialternative drift-diffusion model predicts the relationship between visual fixations and choice in value-based decisions. *Proceedings of the National Academy of Sciences*, *108*(33), 13852–13857. https://doi.org/10.1073/pnas.1101328108

Krakauer, J. W., Ghazanfar, A. A., Gomez-Marin, A., MacIver, M. A., & Poeppel, D. (2017). Neuroscience Needs Behavior: Correcting a Reductionist Bias. *Neuron*, *93*(3), 480–490. https://doi.org/10.1016/j.neuron.2016.12.041

Kravitz, D. J., Saleem, K. S., Baker, C. I., Ungerleider, L. G., & Mishkin, M. (2013). The ventral visual pathway: An expanded neural framework for the processing of object quality. *Trends in Cognitive Sciences*, *17*(1), 26–49. https://doi.org/10.1016/j.tics.2012.10.011

Leong, Y. C., Radulescu, A., Daniel, R., DeWoskin, V., & Niv, Y. (2017). Dynamic Interaction between Reinforcement Learning and Attention in Multidimensional Environments. *Neuron*, *93*(2), 451–463. https://doi.org/10.1016/j.neuron.2016.12.040

Lim, S.-L., O'Doherty, J. P., & Rangel, A. (2011). The Decision Value Computations in the vmPFC and Striatum Use a Relative Value Code That is Guided by Visual Attention. *Journal of Neuroscience*, *31*(37), 13214–13223. https://doi.org/10.1523/JNEUROSCI.1246-11.2011

Liu, H.-Z., Lyu, X.-K., Wei, Z.-H., Mo, W.-L., Luo, J.-R., & Su, X.-Y. (2021). Exploiting the dynamics of eye gaze to bias intertemporal choice. *Journal of Behavioral Decision Making*, *34*(3), 419–431. https://doi.org/10.1002/bdm.2219

Liu, H.-Z., Zhou, Y.-B., Wei, Z.-H., & Jiang, C.-M. (2020). The power of last fixation: Biasing simple choices by gaze-contingent manipulation. *Acta Psychologica*, *208*, 103106. https://doi.org/10.1016/j.actpsy.2020.103106

Manohar, S. G., & Husain, M. (2013). Attention as foraging for information and value. *Frontiers in Human Neuroscience*, *7*. https://doi.org/10.3389/fnhum.2013.00711

McGinty, V. B., & Lupkin, S. M. (2021). Value signals in orbitofrontal cortex predict economic decisions on a trial-to-trial basis. *BioRxiv*, 2021.03.11.434452. https://doi.org/10.1101/2021.03.11.434452

McGinty, V. B., Rangel, A., & William T. Newsome. (2016). Orbitofrontal Cortex Value Signals Depend on Fixation Location during Free Viewing. *Neuron*, *90*(6), 1299–1311. https://doi.org/10.1016/j.neuron.2016.04.045

Molter, F., Thomas, A. W., Heekeren, H. R., & Mohr, P. N. C. (2019). GLAMbox: A Python toolbox for investigating the association between gaze allocation and decision behaviour. *BioRxiv*, 741678. https://doi.org/10.1101/741678

Moore, T., & Armstrong, K. M. (2003). Selective gating of visual signals by microstimulation of frontal cortex. *Nature*, *421*(6921), Article 6921. https://doi.org/10.1038/nature01341

Moore, T., & Fallah, M. (2004). Microstimulation of the Frontal Eye Field and Its Effects on Covert Spatial Attention. *Journal of Neurophysiology*, *91*(1), 152–162. https://doi.org/10.1152/jn.00741.2002

National Research Council (US) Committee for the Update of the Guide for the Care and Use of Laboratory Animals. (2011). *Guide for the Care and Use of Laboratory Animals* (8th ed.). National Academies Press (US). http://www.ncbi.nlm.nih.gov/books/NBK54050/

Neggers, & Bekkering. (2001). Gaze Anchoring to a Pointing Target Is Present During the Entire Pointing Movement and Is Driven by a Non-Visual Signal. *Journal of Neurophysiology*, *86*(2), 961–970. https://doi.org/10.1152/jn.2001.86.2.961

Neggers, S. F., & Bekkering, H. (2000). Ocular gaze is anchored to the target of an ongoing pointing movement. *Journal of Neurophysiology*, *83*(2), 639–651. https://doi.org/10.1152/jn.2000.83.2.639

Öngür, D., & Price, J. L. (2000). The Organization of Networks within the Orbital and Medial Prefrontal Cortex of Rats, Monkeys and Humans. *Cerebral Cortex*, *10*(3), 206–219. https://doi.org/10.1093/cercor/10.3.206

Padoa-Schioppa, C., & Assad, J. A. (2006). Neurons in the orbitofrontal cortex encode economic value. *Nature*, *441*(7090), 223–226. https://doi.org/10.1038/nature04676

Pärnamets, P., Johansson, P., Hall, L., Balkenius, C., Spivey, M. J., & Richardson, D. C. (2015). Biasing moral decisions by exploiting the dynamics of eye gaze. *Proceedings of the National Academy of Sciences*, *112*(13), 4170–4175. https://doi.org/10.1073/pnas.1415250112

Paton, J. J., Belova, M. A., Morrison, S. E., & Salzman, C. D. (2006). The primate amygdala represents the positive and negative value of visual stimuli during learning. *Nature*, *439*(7078), 865–870. https://doi.org/10.1038/nature04490

Pisauro, M. A., Fouragnan, E., Retzler, C., & Philiastides, M. G. (2017). Neural correlates of evidence accumulation during value-based decisions revealed via simultaneous EEG-fMRI. *Nature Communications*, *8*, 15808. https://doi.org/10.1038/ncomms15808

Ratcliff, R., & McKoon, G. (2008). The diffusion decision model: Theory and data for two-choice decision tasks. *Neural Computation*, *20*(4), 873–922.

Resulaj, A., Kiani, R., Wolpert, D. M., & Shadlen, M. N. (2009). Changes of mind in decision-making. *Nature*, *461*(7261), 263–266. https://doi.org/10.1038/nature08275

Reyes-Puerta, V., Philipp, R., Lindner, W., & Hoffmann, K.-P. (2010). Role of the Rostral Superior Colliculus in Gaze Anchoring During Reach Movements. *Journal of Neurophysiology*, *103*(6), 3153–3166. https://doi.org/10.1152/jn.00989.2009

Rich, E. L., & Wallis, J. D. (2016). Decoding subjective decisions from orbitofrontal cortex. *Nature Neuroscience*, *19*(7), 973–980. https://doi.org/10.1038/nn.4320

Rodriguez, C. A., Turner, B. M., Van Zandt, T., & McClure, S. M. (2015). The neural basis of value accumulation in intertemporal choice. *European Journal of Neuroscience*, *42*(5), 2179–2189. https://doi.org/10.1111/ejn.12997

Ruff, C. C., Blankenburg, F., Bjoertomt, O., Bestmann, S., Freeman, E., Haynes, J.-D., Rees, G., Josephs, O., Deichmann, R., & Driver, J. (2006). Concurrent TMS-fMRI and Psychophysics Reveal Frontal Influences on Human Retinotopic Visual Cortex. *Current Biology*, *16*(15), 1479–1488. https://doi.org/10.1016/j.cub.2006.06.057

Silvanto, J., Lavie, N., & Walsh, V. (2006). Stimulation of the Human Frontal Eye Fields Modulates Sensitivity of Extrastriate Visual Cortex. *Journal of Neurophysiology*, *96*(2), 941–945. https://doi.org/10.1152/jn.00015.2006

Smith, S. M., & Krajbich, I. (2018). Attention and choice across domains. *Journal of Experimental Psychology: General*, *147*(12), 1810–1826. https://doi.org/10.1037/xge0000482

Smith, S. M., & Krajbich, I. (2019). Gaze Amplifies Value in Decision Making. *Psychological Science*, *30*(1), 116–128. https://doi.org/10.1177/0956797618810521

Stuphorn, V., Bauswein, E., & Hoffmann, K.-P. (2000). Neurons in the Primate Superior Colliculus Coding for Arm Movements in Gaze-Related Coordinates. *Journal of Neurophysiology*, *83*(3), 1283–1299. https://doi.org/10.1152/jn.2000.83.3.1283

Sui, X.-Y., Liu, H.-Z., & Rao, L.-L. (2020). The timing of gaze-contingent decision prompts influences risky choice. *Cognition*, *195*, 104077. https://doi.org/10.1016/j.cognition.2019.104077

Tavares, G., Perona, P., & Rangel, A. (2017). The Attentional Drift Diffusion Model of Simple Perceptual Decision-Making. *Frontiers in Neuroscience*, *11*. https://doi.org/10.3389/fnins.2017.00468

Taylor, P. C. J., Nobre, A. C., & Rushworth, M. F. S. (2007). FEF TMS Affects Visual Cortical Activity. *Cerebral Cortex*, *17*(2), 391–399. https://doi.org/10.1093/cercor/bhj156

Thomas, A. W., Molter, F., Krajbich, I., Heekeren, H. R., & Mohr, P. N. C. (2019). Gaze bias differences capture individual choice behaviour. *Nature Human Behaviour*. https://doi.org/10.1038/s41562-019-0584-8

Vaidya, A. R., & Fellows, L. K. (2015). Ventromedial Frontal Cortex Is Critical for Guiding Attention to Reward-Predictive Visual Features in Humans. *Journal of Neuroscience*, *35*(37), 12813–12823. https://doi.org/10.1523/JNEUROSCI.1607-15.2015

Vehtari, A., Gelman, A., & Gabry, J. (2017). Practical Bayesian model evaluation using leave-one-out cross-validation and WAIC. *Statistics and Computing*, *27*(5), 1413–1432. https://doi.org/10.1007/s11222-016-9696-4

Westbrook, A., van den Bosch, R., Määttä, J. I., Hofmans, L., Papadopetraki, D., Cools, R., & Frank, M. J. (2020). Dopamine promotes cognitive effort by biasing the benefits versus costs of cognitive work. *Science*, *367*(6484), 1362–1366. https://doi.org/10.1126/science.aaz5891

Whitney, D., & Levi, D. M. (2011). Visual crowding: A fundamental limit on conscious perception and object recognition. *Trends in Cognitive Sciences*, *15*(4), 160–168. https://doi.org/10.1016/j.tics.2011.02.005

Wise, S. P. (2008). Forward frontal fields: Phylogeny and fundamental function. *Trends in Neurosciences*, *31*(12), 599–608. https://doi.org/10.1016/j.tins.2008.08.008

Xie, Y., Nie, C., & Yang, T. (n.d.). *Covert shift of attention modulates the value encoding in the orbitofrontal cortex*. 21.

Supplemental Material

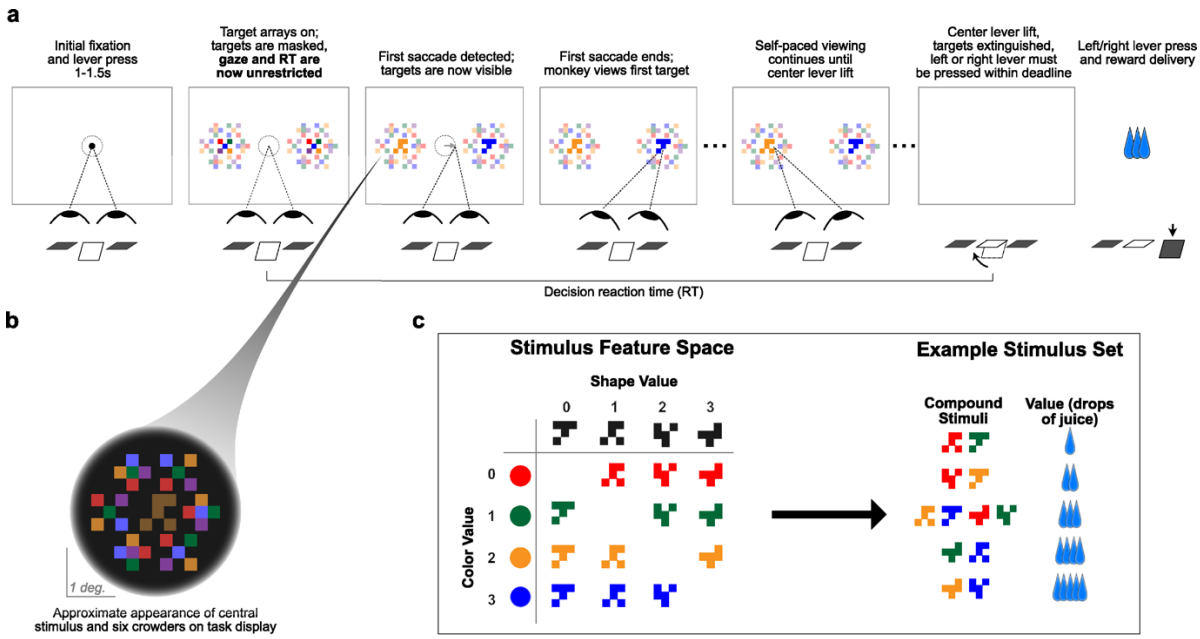

Figure S1. Full task sequence **A.** Illustration of the complete task sequence. Note that for illustration purposes, in this panel the background is white, and the surrounding crowders are shown at reduced saturation relative to the centrally located targets. However, on the actual task display, the background was dark, and target luminance was reduced relative to the crowders (see panel B). **B.** Close-up view of a single target array, consisting of a central yellow choice target surrounded by six non-task-relevant crowders. Two such arrays appear on the display (panel A), each centered 7.5° from the display center. **C.** To generate stimulus sets, four shapes are selected without replacement from 7 possible; then each is rotated randomly by 0, 90, 180, 270 degrees. The four rotated shapes are then combined with four colors selected randomly from equally-spaced points on a color wheel defined within the RGB gamut in the CIELUV color space. The grid on the left shows the color and shape primitives as rows and columns, respectively. Each primitive was assigned a value from 0 to 4, corresponding to the number of drops of juice each would signal on its own. The 12 targets that made up a given stimulus set were taken from the off-diagonal of this grid; their value was determined according to their shape and color. The result is a set of targets ranging in value from 1 to 5 drops of juice.

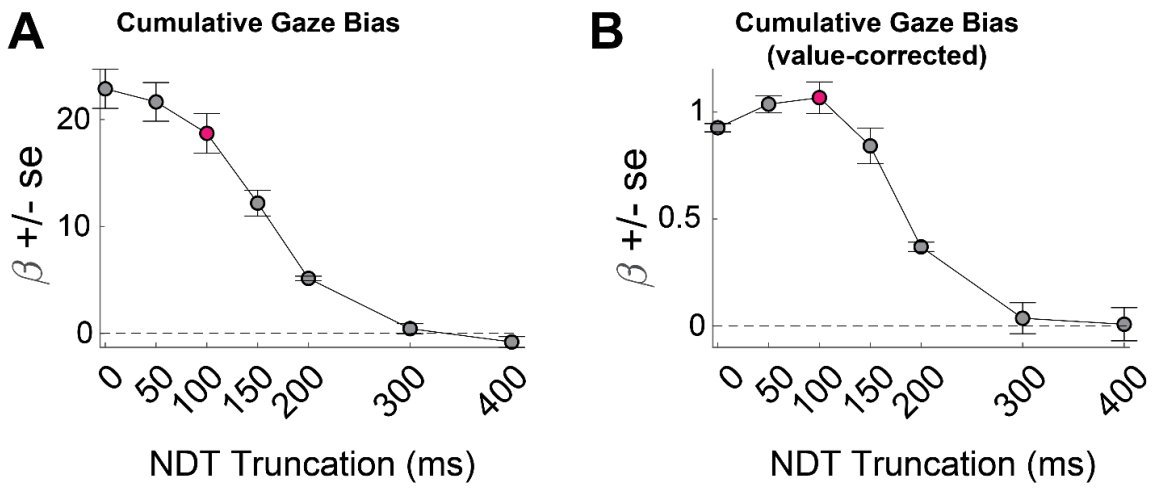

Supplemental Figure S2. The effect of NDT truncation on the cumulative gaze bias. Beta values in A and B refer to the estimate for variable time-advantage in Table 1, rows 15 and 16 (respectively), with standard errors derived from the mixed-effects model.

1091

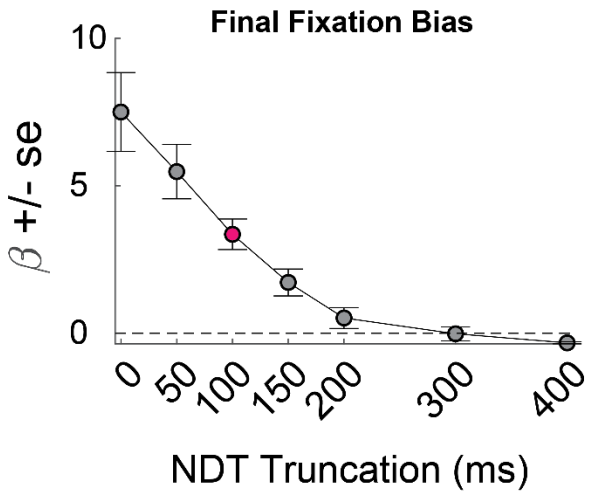

Supplemental Figure S3. The effect of NDT truncation on the final fixation bias. Beta value refers to the estimate for variable last-is-left Table 1, row 17, with standard errors derived from the mixed-effects model.

	Monkey C		Monkey K	
	Bias Model	No Bias Model	Bias Model	No Bias Model
γ - MAP	0.089	1 (fixed)	-0.061	1 (fixed)
HPD 2.5	0.064	1 (fixed)	-0.081	1 (fixed)
HPD 97.5	0.12	1 (fixed)	-0.031	1 (fixed)
σ - MAP	0.2	0.21	0.17	0.21
HPD 2.5	0.19	0.2	0.17	0.2
HPD 97.5	0.2	0.21	0.17	0.21
□ - MAP	0.27	0.19	0.31	0.2
HPD 2.5	0.26	0.18	0.3	0.2
HPD 97.5	0.27	0.19	0.31	0.21
ν - MAP	2.31	2.35	2.2	2.27
HPD 2.5	2.3	2.34	2.2	2.26
HPD 97.5	2.32	2.36	2.21	2.28
WAIC	-15396.92	-12039.05	-18570.93	-10411.22
Std. Error	246.87	247.02	232.64	224.5

Table S1. Parameter estimates from both GLAM variants. *Maximum a posteriori (MAP) and 97.5 highest posterior density (HPD) interval for each parameter obtained from fitting each variant to all data available for each monkey. Note that for "Bias Model",* **γ** *was a free parameter in the model, while in the "No Bias Model",* **γ** *was fixed at 1.* **γ**, *gaze bias parameter;* **σ**, *noise parameter;* **τ,** *logistic scaling parameter;* **ν**, *velocity parameter.* ***WAIC,*** *widely applicable information criteria. See Methods for further details on parameter definitions.*

	WAIC (Std. Error)	
NDT Truncation	Multiplicative Model	Additive Model
0ms	-40791.81 (343.35)	-40040.03 (338.1)
50ms	-36661.06 (341.38)	-35839.78 (341.39)
100ms*	-33072.05 (344.92)	-31762.69 (344.59)
150ms*	-30849.61 (353.41)	-29069.38 (352.34)
200ms*	-30168.18 (368.04)	-27779.11 (366.18)
300ms*	-26680.32 (390.3)	-24203.94 (392.17)
400ms*	-24138.04 (363.27)	-23070.16 (361.39)

Table S2. Effect of NDT truncation on relative fit of the GLAM with either an additive or a multiplicative gaze term. Table entries give the WAIC with standard errors in parentheses * *indicates models where the standard errors for the two models do not overlap, indicating the fits are statistically different from each other.*

Metric	Estimate	Confidence Interval	*p*-Value	Figure
Choice (1 = left, 0 = right)	-0.041	[-0.12, 0.042]	0.33	9 A/D
Reaction Time	0.00075	[-0.0034, 0.0012]	0.57	9 B/E
Value-corrected choice probability	-5.71E-17	[-0.0060, 0.0060]	1	9 C/F

Table S3. Comparison of GLAM simulations to held out trials. *Estimates and confidence intervals are the result of mixed effects models where each metric was regressed against a binary variable indicating whether the data were from the predicted trials or the observed trials. Confidence intervals including zero indicate no significant difference between predicted vs. observed, i.e. that the predicted data are a good fit to out of sample observations. The choice metric was assessed using a logistic regression. The others were linear. All models included "Monkey" as a random effect. p-values were obtained from an ANOVA on the output of the mixed effects regressions.*